Free Radical Biology and Medicine xxx (xxxx) xxx–xxx

Contents lists available at ScienceDirect

Free Radical Biology and Medicine

journal homepage: www.elsevier.com/locate/freeradbiomed

Original article

Trans-4,4′-dihydroxystilbene ameliorates cigarette smoke-induced progression of chronic obstructive pulmonary disease via inhibiting oxidative stress and inflammatory response

Tian Wang[a,1], Fang Dai[b,1], Guo-Hui Li[c,1], Xue-Mei Chen[d], Yan-Ru Li[a], Shu-Qi Wang[a], Dong-Mei Ren[a], Xiao-Ning Wang[a], Hong-Xiang Lou[a], Bo Zhou[b], Tao Shen[a,*]

[a] Key Lab of Chemical Biology (MOE), School of Pharmaceutical Sciences, Shandong University, Jinan, People's Republic of China
[b] State Key Lab of Applied Organic Chemistry, Lanzhou University, Lanzhou, People's Republic of China
[c] Department of Pharmacy, Jinan Maternity and Child Care Hospital, Jinan, People's Republic of China
[d] Department of Health Management, Beijing Rehabilitation Hospital, Capital Medical University, Beijing, People's Republic of China

ARTICLE INFO

Keywords:
Chronic obstructive pulmonary disease
4,4′-Dihydroxystilbene
Inflammatory response
NF-κB
Nrf2
Oxidative stress

ABSTRACT

Chronic obstructive pulmonary disease (COPD) is a chronic inflammatory disease resulted from airflow obstructions, and there is a driving requirement for novel and effective preventive and therapeutic agents of COPD. Nuclear factor-erythroid 2-related factor 2 (Nrf2) has been regarded to be a promising therapeutic target for COPD. Resveratrol is a natural Nrf2 activator with antioxidant and anti-inflammatory properties, however, its application is limited by its relative low efficiency and poor bioavailability. Herein, based on the skeleton of resveratrol, *trans*-4,4′-dihydroxystilbene (DHS) has been firstly identified to be an Nrf2 activator, which is more potent than the well-known sulforaphane (SF) and resveratrol. Our results indicate that DHS blocks Nrf2 ubiquitylation through specifically reacting with Cys151 cysteine in Keap1 protein to activate Nrf2-regulated defensive response, and thus enhances intracellular antioxidant capability. Furthermore, DHS relieves lipopolysaccharide (LPS)-stimulated inflammatory response via inhibition of NF-κB. Importantly, DHS significantly ameliorates pathological alterations (e.g. infiltration of leukocytes and fibrosis), downregulates the levels of oxidant biomarkers malondialdehyde (MDA) and 8-oxo-7,8-dihydro-2′-deoxyguanosin (8-oxo-dG), and inhibits the overproductions of inflammatory mediators [e.g. tumor necrosis factor *α* (TNF-*α*), cyclooxygenase-2 (COX-2), and matrix metalloproteinase-9 (MMP-9)] in a cigarette smoke (CS)-induced pulmonary impairment mice model. Taken together, this study demonstrates that DHS attenuates the CS-induced pulmonary impairments through inhibitions of oxidative stress and inflammatory response targeting Nrf2 and NF-κB *in vitro* and *in vivo*, and could be developed into a preventive agent against pulmonary impairments induced by CS.

1. Introduction

Chronic obstructive pulmonary disease (COPD) is characterized by persistent and progressive airflow limitation that is associated with an enhanced chronic inflammatory response in the airways, and has been predicted to rank third worldwide in terms of mortality in 2020 [1]. Cigarette smoke (CS), containing approximately 10^{14} relatively long-lived oxidants/free radicals per puff, can induce intracellular oxidative stress, and has been verified to be the predominant cause for this chronic disease. These exogenous oxidants activate redox-sensitive transcription factors [e.g. nuclear transcription factor-κB (NF-κB), and activator protein 1 (AP-1)]), induce the accumulation of inflammatory cells (e.g. macrophages, and neutrophils), promote the release of ROS and pro-inflammatory mediators, and thus stimulate inflammatory response [2,3]. The increased oxidative stress and stimulated inflammatory response form a positive feedback loop, and play a vital role in the pathophysiology of COPD [4]. Therefore, inhibitions of oxidative stress and inflammatory response could prove to be an effective means to improve survival and quality of life and block the pathological process of COPD patients.

The nuclear factor erythroid 2-related factor 2 (Nrf2) is a transcription factor that mounts defensive responses against oxidative insults. Under normal cellular conditions, Nrf2 is maintained at a low level through Keap1-regulated ubiquitylation and subsequent 26S

* Corresponding author. School of Pharmaceutical Sciences, Shandong University, 44 Wenhua Xi Road, Jinan 250012, People's Republic of China.
E-mail address: shentao@sdu.edu.cn (T. Shen).
[1] These authors contributed equally to this work.

https://doi.org/10.1016/j.freeradbiomed.2019.11.026
Received 26 September 2019; Received in revised form 17 November 2019; Accepted 18 November 2019

Abbreviations

ARE	antioxidant response element
As(III)	sodium arsenite
BALF	bronchoalveolar lavage fluid
CHX	cycloheximide
COPD	chronic obstructive pulmonary disease
COX-2	cyclooxygenase-2
CS	cigarette smoke
Dex	dexamethasone
DHS	*trans*-4,4′-dihydroxystilbene
GCLM	glutamate-cysteine ligase regulatory subunit
GSH	glutathione
IκB	inhibitors of κB
IKK	IκB kinase
ILs	interleukins
iNOS	inducible nitric oxide synthase
LPS	lipopolysaccharide
MDA	malondialdehyde
MMPs	matrix metalloproteinases
NQO1	NAD(P)H quinone oxidoreductase 1
NF-κB	nuclear transcription factor-κB
Nrf2	nuclear factor-erythroid 2-related factor 2
8-oxo-dG	8-oxo-7,8-dihydro-2′-deoxyguanosin
PPI	protein-protein interaction
RNS	reactive nitrogen species
ROS	reactive oxygen species
R. T.	room temperature
RT-PCR	real-time reverse transcription-polymerase chain reaction
SF	sulforaphane
tBHQ	tert-butylhydroquinone
TGF-β1	transforming growth factor-β1
TNF-*α*	tumor necrosis factor *α*

proteasome-regulated degradation. When the intracellular redox imbalance emerges, Nrf2 translocates into the nucleus, binds to the antioxidant response element (ARE) located in the promoter region of cytoprotective genes, and increases their transcription [5]. These Nrf2 target genes include intracellular antioxidant enzymes [e.g. glutamate-cysteine ligase regulatory subunit (GCLM)], and phase II detoxifying enzymes [e.g. NAD(P)H: quinone oxidoreductase 1 (NQO1)], which maintain the intracellular redox balance and promote excretion of toxicants [6].

NF-κB is a redox-sensitive transcription factor that is involved in the regulation of genes in response to inflammatory stimuli [2]. Under basal conditions, NF-*κ*B is sequestered by inhibitors of *κ*B (I*κ*B) proteins in the cytoplasm. Upon cell stimulation, IκB is phosphorylated by IκB kinase (IKK) to release NF-*κ*B into the nucleus that driving the expressions of inflammation-related genes. These inflammatory genes include proinflammatory cytokines [e.g. tumor necrosis factor *α* (TNF-*α*) and interleukins (ILs)], chemokines, and inflammation-related proteins [e.g. cyclooxygenase-2 (COX-2), matrix metalloproteinases (MMPs), and inducible nitric oxide synthase (iNOS)] [7].

The essential roles of Nrf2 and NF-κB in the progression of COPD have been well documented. Nrf2-deficient mice were highly susceptible to CS-induced emphysema [8]. Lung tissues and alveolar macrophages from COPD patients demonstrated a declined expression of Nrf2 [9]. Furthermore, NF-κB pathway was activated in macrophages and epithelial cells of COPD patients [10,11]. Therefore, given the biological functions of Nrf2 and NF-κB, molecules with the capabilities of activating Nrf2-mediated antioxidant responses and inhibiting NF-κB-regulated inflammatory response are potential preventive and therapeutic agents against COPD [12,13].

Resveratrol is a naturally derived constituent distributed in grape, red wine, and some folk medicines, and has displayed diverse bioactivities and potential medical applications, covering anticancer, antioxidant, anti-inflammatory, neuroprotective, antidiabetic, and cardiovascular properties [14–17]. A growing body of evidence implied that the therapeutic potential against human diseases (e.g. lung disease, diabetic nephropathy) was associated with its induction on Nrf2-mediated defensive response [18–21]. Our data have verified that resveratrol was capable of inducing Nrf2 signaling pathway through upregulating mRNA and protein levels of Nrf2 (Fig. 1A and Fig. S1 in Supporting Materials). Compared with the potency of the well-known Nrf2 activator sulforaphane (SF), resveratrol demonstrates weak Nrf2 inducing effect, yet it is still a promising leading compound for design and discovery of new preventive and therapeutic agents.

To find potent resveratrol-based Nrf2 activators, chemical synthesis and modification of resveratrol analogues have been performed, and resulted in the discovery of a potent Nrf2 activator *trans*-4,4′-dihydroxystilbene (DHS, **A3**, Fig. 1C). Our results indicate that DHS enhances antioxidant capability through activating Nrf2, and suppresses inflammatory response through inhibiting NF-κB *in vitro* and *in vivo*. Importantly, DHS significantly ameliorates pathological alterations in a CS-induced pulmonary impairment mice model *in vivo*.

2. Materials and methods

2.1. Chemicals and reagents

Resveratrol analogues were synthesized by our lab with a purity > 95%. L-glutamine was purchased from Solarbio (Beijing, China). TEMED, 4% paraformaldehyde, Tween-20, Triton X-100, β-mercaptoethanol, and glycerol were obtained from Dingguo (Beijing, China). Bovine serum albumin (BSA), glycine, 3-(4, 5-dimethylthiazol-2-yl)-2,5-diphenyltetrazoliumbromide (MTT), acrylamide, cycloheximide (CHX), penicillin-streptomycin solution (100X), and sodium dodeeyl sulfate (SDS) were provided by Genview (TX, USA). RPMI1640 and DMEM were offered by Gibco (CA, USA). Lipopolysaccharide (LPS), tert-butylhydroquinone (tBHQ), and sulforaphane (SF) were supplied by Sigma-Aldrich (MO, USA). Didox and MG132 were products of MedChemExpress (NJ, USA). Lipofectamine 2000 was purchased from Invitrogen (CA, USA).

2.2. Cell culture

Normal human lung epithelial Beas-2B cells, human breast carcinoma MDA-MB-231 cells, and RAW 264.7 murine macrophages were obtained from American Type Culture Collection (USA). Beas-2B cells and MDA-MB-231 cells were maintained in RPMI1640 complete medium. RAW 264.7 macrophages were cultivated in DMEM complete medium. All medium included 10% FBS, 0.29 g/L L-glutamine and penicillin-streptomycin (100 units/mL for penicillin and 100 μg/mL for streptomycin, respectively). All of cells were cultivated in a humidified incubator with 5% CO_2 at 37 °C.

2.3. Cell viability assay

The MTT assay was utilized to determine the cell viability. Beas-2B cells (8×10^3 cells/well), MDA-MB-231 cells (1×10^4 cells/well) and RAW 264.7 cells (8×10^4 cells/well) were seeded in the 96-well plates for overnight incubation, and exposed to different doses of DHS for indicated time. 20 μL of MTT solution was added into each well. After further incubating 3 h, the supernatant was decanted carefully, and precipitate was dissolved in 100 μL DMSO. Then, the plates were shaken at room temperature (R.T.) for 10 min. The absorbance was

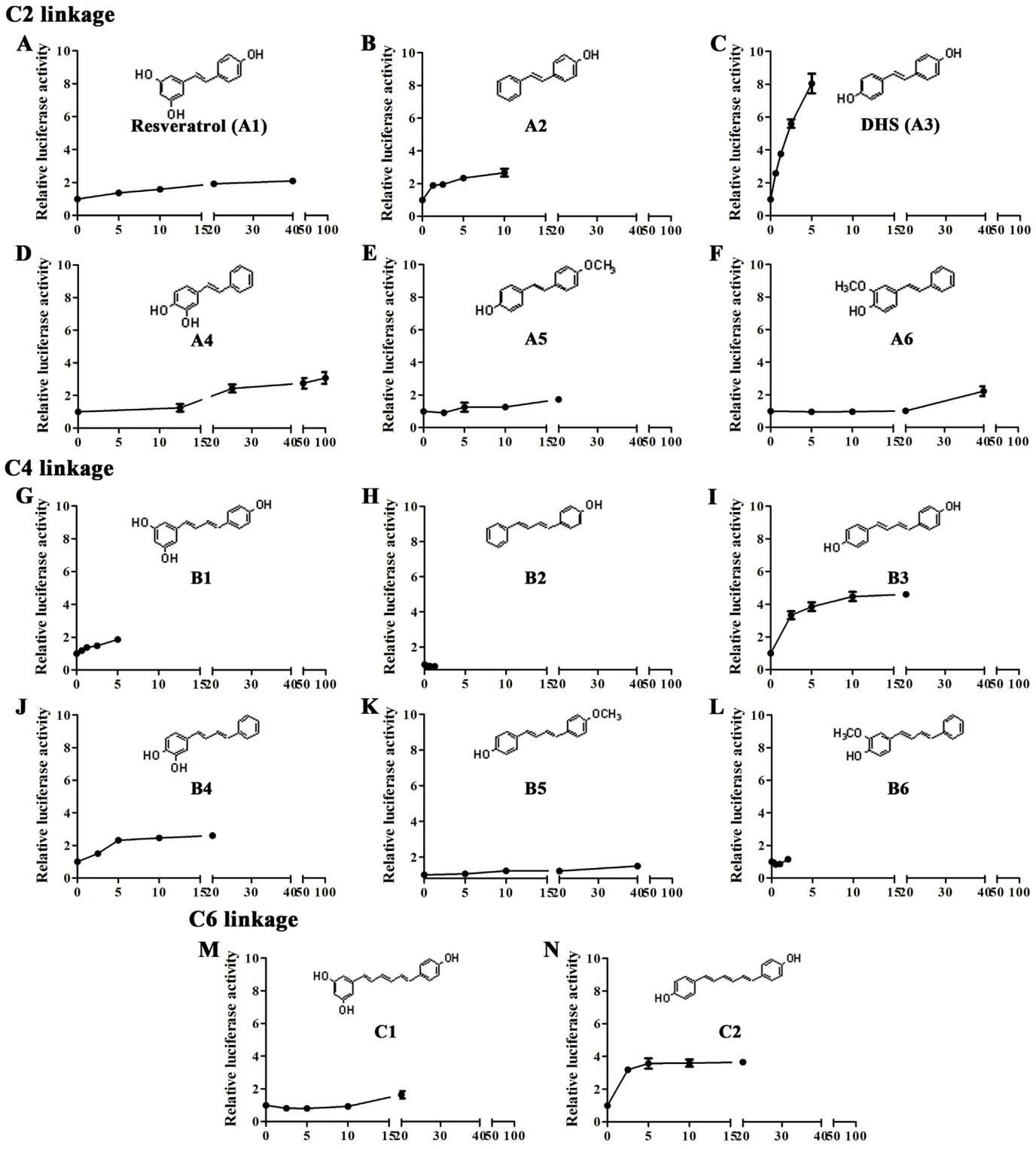

Fig. 1. Identification of resveratrol analogues as potential Nrf2 activators. The stable MDA-MB-231 cell line expressing ARE-luciferase was used for evaluating Nrf2 induction. Cells were treated with the indicated doses of resveratrol analogues (μM) for 16 h before luciferase activities were measured. SF (2.5 μM) was used as a positive control, and displayed an approximately 2.6-fold induction of ARE luciferase assay. Results are expressed as mean ± SD (n = 3).

detected at 570 nm using the Model 680 plate reader (Bio-Rad, CA, USA).

2.4. Luciferase reporter gene assay

A stable ARE luciferase reporter cell line MDA-MB-231-ARE-Luc was used for identification of Nrf2 inducing effects of resveratrol and its analogues. The cells were treated with several doses of tested compounds for 16 h, and the luciferase activity was measured on the Synergy 2 plate reader (BioTeK, USA). For the dual luciferase reporter gene assay, RAW 264.7 cells or Beas-2B cells were seeded in 24-well plates. The NF-κB luciferase plasmid or ARE-luciferase plasmid was cotransfected with the renilla luciferase plasmid using lipofectamine 2000 (Invitrogen, CA, USA) after reaching 70%–90% density. After

transfection, Beas-2B cells were treated with different doses of DHS for 18 h. RAW 264.7 cells were pretreated with indicated doses of DHS for 1 h, followed by cotreatment with DHS and LPS (1 μg/ml) for additional 16 h. Then, the Promega dual-luciferase reporter gene assay system (WI, USA) was applied to determine firefly and renilla luciferase activities.

2.5. Immunoblot analysis

Cells were seeded in D35 dishes at an appropriate density and exposed to DHS for indicated time. Then cells were collected to extract the total protein. The lung tissue was weighed and homogenized in pre-cold sample buffer (1 g of the tissue in 9 mL of sample buffer). After centrifuging at 10,000 rpm for 10 min, the supernatant was taken for the preparation of total tissue protein. Briefly, cells were lysed with sample buffer consisting of 10 mL β-mercaptoethanol, 2% SDS, 10% glycerol, 50 mM Tris-HCl (pH 6.8) and 0.05 g bromophenol blue, and the lung tissues were lysed with sample buffer without bromophenol blue. The obtained proteins were separated using SDS-PAGE on 7.5% or 10% gel, blotted onto a nitrocellulose membrane (Millipore, MA, USA). The membrane was probed with different indicated primary antibodies overnight at 4 °C followed by horseradish peroxidase (HRP)-conjugated secondary antibodies at R.T. for 1 h. The protein bands were visualized by Bio-Rad ChemiDoc XRS + system (CA, USA) using ECL reagents. Chemiluminescent signal was quantified with Image J analyze system.

2.6. Immunofluorescence

RAW 264.7 cells or Beas-2B cells were seeded in D35 dishes which have been pre-placed with cell climbing pieces. After exposure to the specified concentration of DHS for appropriate time, cells were fixed for 10 min with pre-cooled acetone/methanol (1:1). After rinsing, the cell climbing pieces were exposed to primary antibodies against NF-κB p65 (1:500) or Nrf2 (1:500) overnight at 4 °C, and followed by Alexa Flour 594 (1:300) for 2 h at R.T. The nuclei were stained for 10 min with DAPI (2.5 μg/mL) in the darkness. The images of NF-κB or Nrf2 with DAPI staining were observed by BX53 + DP73 fluorescence microscope (Tokyo, Japan).

2.7. Nrf2 protein half-life measurement

Beas-2B cells were seeded in ten D35 dishes. The cells in drug treatment groups or blank groups were treated or untreated with DHS for 8 h. Afterwards, the cells were exposed to 50 μM CHX. Nrf2 proteins were harvested at 0, 10, 20, 30, 40 min, respectively, and were subjected to immunoblot analysis.

2.8. Reduced glutathione (GSH) assay

Beas-2B cells were seeded in D60 dishes. After reaching the appropriate density, different doses of DHS were added to corresponding dishes for 24 h, or indicated dose of DHS was added to corresponding dishes for different time. Reduced GSH assay kits (Jiancheng Bioengineering Institute, Nanjing, China) were used to detect the contents of intracellular reduced GSH following the manufacturer's instructions.

2.9. ROS detection

The content of intracellular ROS was detected with ROS kits (Keygen Biotech, Nanjing, China). Beas-2B cells in D35 dishes were pretreated with indicated dose of DHS for 8 h followed by cotreatment with DHS and 5 μM As (III) for additional 16 h. The medium was removed, and 1 mL serum-free medium containing DCFHDA (10 μM) was added and incubated for additional 20 min. After rinsing, the cells were harvested and resuspended with PBS. ROS content was detected with the fluorescence intensity of DCF at 530 nm after excitation at 488 nm on FACSCelesta flow cytometer (BD Biosciences, CA, USA). Meanwhile, the fluorescence signals were photographed with an Olympus BX53 + DP73 fluorescence imaging system (Tokyo, Japan).

2.10. Nuclear and cytoplasmic extraction

Nuclear and cytoplasmic proteins were collected with nuclear and cytoplasmic protein extraction kit (Sangon Biotech, Shanghai, China). RAW 264.7 cells and Beas-2B cells were seeded in D60 dishes. After reaching appropriate density, RAW 264.7 cells were pretreated with indicated doses of DHS for 1 h, followed by cotreatment with DHS and LPS (1 μg/ml) for additional 3 h, Beas-2B cells were treated with indicated doses of DHS for 8 h. Proteins were separated according to the protocols of manufacturer. The level of Nrf2 protein in nucleus and cytoplasm was subsequently detected by immunoblot analysis.

2.11. Ubiquitylation analysis

Beas-2B cells were cotransfected with Keap1, Nrf2 and hemagglutinin (HA)-ubiquitin plasmids using Lipofectamine 2000 for 36 h, and then incubated with or without DHS (4 μM) and SF (2 μM), together with proteasome inhibitor MG132 for 6 h. The lysates consisting of 1 mM DTT, 10 mM Tris-HCl, 150 mM NaCl and 2% SDS were used to lyse the cells. 30 μL of supernatant was subjected to immunoblot analysis to evaluate the expression of Nrf2. Four-fold of the buffer containing 10 mM Tris-HCl, 150 mM NaCl and 1% Triton X-100 was added to the residual supernatant. Then antibodies against IgG and Nrf2 (Proteintech Group, IL, USA), protein A beads (Santa Cruz Biotechnology, CA, USA) were added to the mixture, the precipitates were washed and analyzed by immunoprecipitation.

2.12. Measurement of NO production

RAW 264.7 cells (8×10^4 cells/well) were evenly seeded in the 96-well plates for overnight incubation, and exposed to indicated concentrations of DHS or Didox, together with LPS (1 μg/mL) for 24 h. 100 μL of supernatants were mixed with the100 μL of the Griess reagent (1% sulfanilamide, 0.1% naphthylethylenediamine, and 5% phosphoric acid) and incubated for 10 min at R. T. The absorbance was detected at a wavelength of 570 nm using the Model 680 plate reader (Bio-Rad, CA, USA). $NaNO_2$ was used to build a standard curve.

2.13. Enzyme-linked immunosorbent assay (ELISA)

RAW 264.7 cells were seeded in D35 dishes and pretreated with indicated doses of DHS for 1 h, followed by cotreatment with DHS and LPS (1 μg/mL) for additional 16 h. The contents of cytokine in the culture media were measured using ELISA kits (Shanghai Enzyme-linked Biotechnology Co., Ltd., China) following the manufacturer's instructions.

2.14. Real-time reverse transcription-polymerase chain reaction (RT-PCR)

Beas-2B cells or RAW 264.7 cells were seeded into D35 dishes for indicated time, and treated with different doses of DHS for 18 h for Beas-2B cells or pretreated with indicated doses of DHS for 1 h, followed by cotreatment with DHS and LPS (1 μg/ml) for additional 16 h for RAW 264.7 cells. Total RNA was gathered with RNAiso Blood (Takara Bio Inc., Shiga, Japan) following the instructions. Equal amount of total RNA (1 μg) was reverse transcribed into cDNA by PrimeScript™ RT Reagent Kits with gDNA Eraser (Takara Bio Inc., Shiga, Japan). Primer were synthesized by Sangon Biotech (Shanghai, China) and the sequences are as follows: hNrf2, forward (5′-ACACGG TCCACAGCTCATC-3′) and reverse (5′-TGTCAATCAAATCCATGTC CTG-3′); hNQO1, forward (5′-ATGTATGACAAAGGACCCTTCC-3′) and

reverse (5′-TCCCTTGCAGAGAGTACATGG-3′); hGCLM, forward (5′-GACAAAACACAGTTGGAACAGC-3′) and reverse (5′-CAGTCAAATC TGGTGGCATC-3′); hKeap1, forward (5′-ACCACAACAGTGTGGAGA GGT-3′) and reverse (5′-CGATCCTTCGTGTCAGCAT-3′); hGAPDH, forward (5′-CTGACTTCAACAGCGACACC-3′) and reverse (5′-TGCTGTAG CCAAATTCGTTGT-3′); miNOS, forward (5′-CAAGAGTTTGACCAGAGG ACC-3′) and reverse (5′-TGGAACCACTCGTACTTGGGA-3′); mTNF-α, forward (5′-TTGACCTCAGCGCTGAGTTG-3′) and reverse (5′-CCTGTA GCCCACGTCGTAGC-3′); mIL-1β, forward (5′-CAGGATGAGGACATGA GCACC-3′) and reverse (5′-CTCTGCAGACTCAAACTCCAC-3′); mCOX-2, forward (5′-CACTACATCCTGACCCACTT-3′) and reverse (5′-ATGCTCC TGCTTGAGTATGT-3′); mMMP-9, forward (5′-GCTGACTACGATAAGG ACGGCA-3′) and reverse (5′-GCGGCCCTCAAAGATGAACGG-3′); mIL-6, forward (5′-GTACTCCAGAAGACCAGAGG-3′) and reverse (5′-TGCTGG TGACAACCACGGCC-3′); mβ-Actin, forward (5′-CGCTCATTGCCGATA GTGAT-3′) and reverse (5′-TGTTTGAGACCTTCAACACC-3′). RT-PCR was carried out using TB Green™ Premix Ex Taq™ (Takara Bio Inc., Shiga, Japan) and primer. The data obtained was relative mRNA levels normalized to GAPDH or β-actin.

2.15. In vivo model establishment and drug administration

36 male C57BL/6 mice (6–8 weeks, 20–22 g, Animal Center of Shandong University) were used in this research. The animals were maintained under a 12 h day/night cycle with water and regular rodent diet given ad libitum. All *in vivo* experiments complied with the rules of Ethical Committee and Institutional Animal Care and Use Committee of Shandong University. After one-week quarantine adaptation, above mice were assigned to 6 groups randomly for different treatment: the control group, the CS exposure group, the tBHQ group (40 mg/kg), the dexamethasone (Dex) group (1 mg/kg), the low dose group of DHS (2 mg/kg) and the high dose group of DHS (4 mg/kg). Dex, tBHQ and DHS were dissolved with DMSO and further diluted with sterile water to working concentration. Above mice, except those in the control group (exposure to fresh air), were placed in a 18-L perspex chamber, exposed to smoke generated from 5 cigarettes (the exposure to the smoke of one cigarette was 6 min) with a 5 min smoke-free break between exposure to each cigarette. The fresh air was simultaneously delivered into the chamber by a peristaltic pump with a rate of 2 L/min. The mean total suspended particulate mass concentration in the chamber was approximately 524 mg/m^3 recorded by a MicroDust Monitor. CS-exposed mice had a carboxyhemoglobin (HbCO) level of 11.23% versus mice in control group with a HbCO level of 0.41%. The exposures of mice to CS were performed for a total of 16 weeks (5 days/week). The cigarettes are produced by Hongta Tobacco (group) Co., LTD, Yunnan, China, and the composition of one cigarette smoke were 1.0 mg nicotine, 11 mg CO, and 10 mg tar. The administration of DHS was carried out via an intraperitoneal injection (i.p.) at doses of 2 and 4 mg/kg/d before CS exposure for a total of 16 weeks (4 days/week). Dex (1 mg/kg) and tBHQ (40 mg/kg), as positive control drugs, were given i.p. before CS exposure. Simultaneously, a same volume of vehicle was administered to mice in the control group and CS exposure group in the same way. The procedure for administration and CS exposure per week has been displayed in Fig. 7A. During this period, the body weight was measured every other week. 24 h after the last CS exposure, the mice were executed via cervical dislocation. The lung tissues and bronchoalveolar lavage fluid (BALF) were gathered for subsequent analysis.

2.16. Collection and analysis of serum and BALF

Prior to mice execution, orbital blood was gathered, and subsequently centrifuged at 2500 rpm for 15 min. The supernatant of serum was subjected to further analysis of cytokines. For the collection of BALF, 1 mL of pre-cooled PBS was injected into trachea and retrieved by a tracheal cannula three times after execution, and followed by centrifugation at 1500 rpm for 10 min. The supernatant of BALF was subjected to subsequent cytokine analysis. Levels of cytokines, including TNF-α, IL-6, and IL-1β were measured using ELISA kits (Shanghai Enzyme-linked Biotechnology Co., Ltd, China) according to the protocols of manufacturer.

2.17. Histopathological evaluation

The right lower lobes of lung tissues were immersed in 4% paraformaldehyde for 24 h, dehydrated and embedded in paraffin. Then, the paraffin-embedded lung tissues were sliced into 4 μm sections. After deparaffinization, the sections were stained with Masson's trichrome, hematoxylin and eosin (H&E) or periodic acid schiff (PAS). The images of sections were observed under 200 X magnification by BX53 + DP73 microscope system (Tokyo, Japan).

2.18. Analysis of lung homogenate

The lung tissues were weighed and homogenized in sterile physiological saline solution (1 g of the tissue in 9 ml of physiological saline). After centrifugation at 10,000 rpm for 10 min, the supernatant was taken for the subsequent measurements. Protein concentrations were detected using a BCA Protein Assay Kit (Beijing Com Win Biotech Co., Ltd., China), and the contents of GSH, and malondialdehyde (MDA) were measured by commercial kits (Jiancheng Bioengineering Institute, Nanjing, China). The levels of 8-oxo-7,8-dihydro-2′-deoxyguanosine (8-oxo-dG) and transforming growth factor-β1 (TGF-β1) were detected by ELISA kits (Shanghai Enzyme-linked Biotechnology Co., Ltd., China) following the manufacturer's instructions.

2.19. Immunohistochemical analysis

The paraffin-embedded lung sections were deparaffinized with xylene followed by rehydration in graded decreasing concentrations of ethanol (100%, 100%, 85%, 75%, 0% and 0%). Antigen retrieval was carried out using a pressure cooker in citrate buffer (pH 6). After rinsing in PBS for 3 times, endogenous peroxidase blocker was added to the sections to block endogenous peroxidase. Then the sections were blocked with normal goat serum, exposed to primary antibodies against Nrf2 (1:500), NF-κB p65 (1:500), TGF-β1 (1:500) and 8-oxo-dG (1:500) overnight at 4 °C, and incubated with reaction enhancer and enzyme-enhanced goat anti-mouse/rabbit IgG polymer at R.T. for 20 min, sequentially. Staining for visualization was executed with a DAB kit following the manufacturer's instructions. The sections were subsequently counterstained with hematoxylin and dehydrated. After sealing with a cover glass, the images of sections were observed under 200 X magnification by BX53 + DP73 microscope system (Tokyo, Japan).

2.20. Statistical analysis

One way analysis of variance (ANOVA) and post hoc multiple comparison Bonferroni test were used to determine the significant difference between two groups in cell-based assay. Kruskal-Wallis test and subsequent Mann-Whitney *U* test were applied for statistical comparisons *in vivo*. Results are presented as the mean ± SD. $P < 0.05$ was considered to be significant.

3. Results

3.1. Identification of resveratrol analogues as potential Nrf2 activators

To find molecules with potent Nrf2 inducing properties, a chemical synthesis and modification of resveratrol-based analogues has been performed. Firstly, the substituents on two aromatic rings were changed to give C2-linkage resveratrol analogues (**A1**–**A6**). Secondly, the two-carbon chain linking the two aromatic rings in resveratrol was modified

to give C4-linkage (**B1–B6**) and C6-linkage (**C1–C2**) resveratrol analogues (Fig. 1). Based on their capability of inducing ARE-luciferase activity, we concluded that resveratrol analogues with 4,4′-dihydroxy substituents on the two aromatic rings, exemplified by DHS (**A3**), **B3** and **C2**, possessed potent Nrf2 inducing effect. Among them, DHS (**A3**) is the most active molecule with 5.6-fold induction of ARE luciferase activity at 2.5 μM, which is stronger than that of SF (2.6-fold induction at 2.5 μM) (Fig. 1C). Therefore, DHS has been selected for the further research on its mechanism and therapeutic potential against COPD.

3.2. DHS enhances intracellular antioxidant capacity in Beas-2B cells

We first evaluated the antioxidant capability of DHS by measuring the effect on reduced GSH in normal lung epithelial Beas-2B cells. As depicted in Fig. 2A, DHS dose-dependently upregulated the level of intracellular reduced GSH, from 0.5 to 4 μM, demonstrating a more potent antioxidant effect than that of SF. Furthermore, it was found that the level of reduced GSH in cells treated by DHS gradually increased from 1 h to 24 h (Fig. 2B). Since As(III) can induce overproduction of ROS [22], we adopted a cell-based oxidative insult model to test the antioxidant property of DHS. DHS (4 μM) significantly attenuated As (III)-induced overproduction of ROS (Fig. 2C–D). Taken together, DHS is able to upregulate the intracellular level of GSH, and inhibit toxicant-induced oxidative stress.

3.3. DHS activates Nrf2-mediated defensive response in Beas-2B cells

The normal human lung epithelial Beas-2B cell line was used to evaluate the capability of DHS on activation of Nrf2-mediated antioxidant response. Consistent with the result observed in MDA-MB-231 cells stably expressing ARE-luciferase (Fig. 1C), the transcriptional activity of Nrf2 was also dose-dependently induced by DHS in an ARE dual luciferase assay (Fig. 3A). We determined the mRNA levels of Nrf2, Keap1, NQO1, and GCLM in Beas-2B cells in response to DHS treatment using qRT-PCR. DHS had no impact on the mRNA levels of Nrf2 and Keap1, but upregulated the NQO1 and GCLM levels (Fig. 3B). As expected, the protein levels of Nrf2 and its regulated genes, NQO1 and GCLM, dose-dependently increased after exposure of cells to DHS for 16 h (Fig. 3C and S2). Next, the time dependent activation of Nrf2 by DHS was conducted. As depicted in Fig. 3D, the protein level of Nrf2 in cells treated by DHS increased as early as 1 h, reached the maximum level at 8 h, and then gradually decreased to the basal level. While the protein levels of NQO1 and GCLM demonstrated sustained upregulation up to 48 h and 24 h, respectively. Translocation of Nrf2 into nucleus is essential for activation of Nrf2-mediated defensive response, and thus Nrf2 nuclear translocation was determined by immunofluorescence and immunoblot assays. DHS evidently promoted Nrf2 nuclear accumulation (Fig. 3E), which was further confirmed by Nrf2 protein level in the cytoplasmic and nuclear fractions (Fig. 3F). More importantly, the potency on induction of the transcription, as well as mRNA and protein expressions of Nrf2 by DHS at doses of 0.5 and 1 μM was comparable to that of SF at 2.5 μM (Fig. 3A–B and S2), suggesting that DHS is more active than the positive control SF. Taken together, DHS is a potent activator which induces expression of Nrf2 target genes by upregulation of Nrf2 at the protein level in Beas-2B cells.

3.4. DHS blocks Nrf2 ubiquitylation and activates Nrf2 in a Keap1-Cys151-dependent manner

The possible mechanism for activation of Nrf2 by DHS was investigated targeting Keap1-mediated ubiquitylation and 26S proteasome-mediated degradation. As displayed in Fig. 4A, DHS (4 μM) significantly blocked ubiquitylation of Nrf2. Accordingly, analysis of the half-life of endogenous Nrf2 protein indicated that it was 13.1 min under the basal condition, and increased to 35.2 min in response to DHS treatment (Fig. 4B). Thus, DHS increased Nrf2 protein stability by suppressing Nrf2 ubiquitylation. DHS-induced suppression of Nrf2 ubiquitylation might be related to the interruption of Nrf2-Keap1

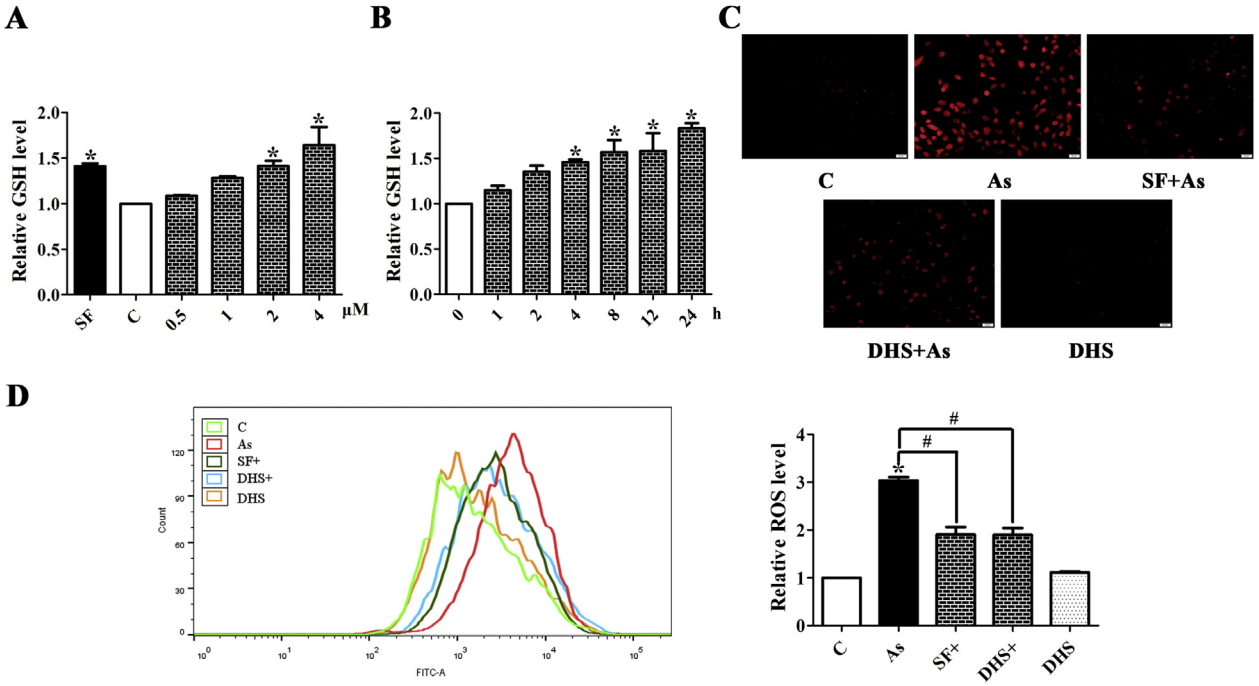

Fig. 2. DHS enhances intracellular antioxidant capacity in Beas-2B cells. (A–B) DHS upregulated the level of intracellular reduced GSH. For A, cells were exposed to the indicated doses of DHS for 24 h, and SF (5 μM) was used as a positive control. For B, cells were exposed to DHS (4 μM) and collected at indicated time. (C–D) DHS attenuated As (III)-induced overproduction of ROS. For C, Beas-2B cells were exposed to 5 μM As (III) for 10 h after 4 μM DHS pretreatment or untreatment for 8 h. For D, Beas-2B cells were exposed to 5 μM As (III) for 16 h after 4 μM DHS pretreatment or untreatment for 8 h. The level of ROS was determined using the ROS detection kits. The scale bar was 20 μm. Results are expressed as mean ± SD (n = 3). $*p < 0.05$ treated versus control; $\#p < 0.05$ treated versus As (III).

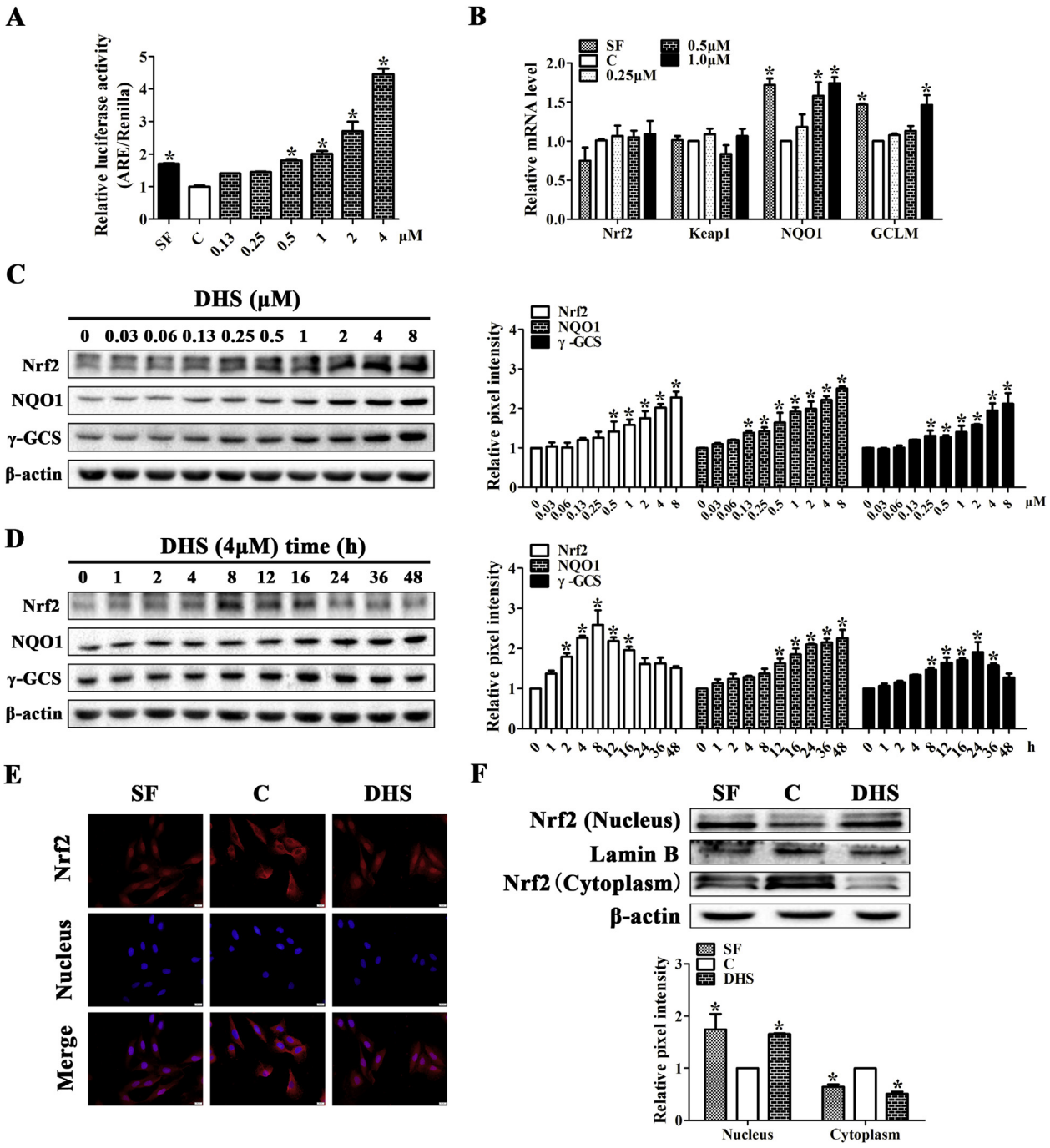

Fig. 3. DHS activates Nrf2-mediated defensive system in Beas-2B cells. (A) DHS induced ARE-luciferase activity in Beas-2B cells. The renilla luciferase plasmid was cotransfected with the ARE-luciferase plasmid using lipofectaine 2000 into Beas-2B cells, and then the cells were exposed to the specified concentrations of DHS for 18 h. (B) DHS upregulated mRNA contents of NQO1 and γ-GCS in Beas-2B cells. Cells were exposed to varying concentrations of DHS for 18 h before extracting mRNA. The mRNA contents were examined with RT-PCR. For A and B, SF (2.5 μM) was used as a positive control. (C) DHS upregulated Nrf2 and the downstream protein. Cells were exposed to various doses of DHS for 16 h, the protein extraction was analyzed by immunoblot analysis. (D) Time course study of DHS on Nrf2-regulated protein expressions. Cells were collected for protein extraction after 4 μM DHS exposure for indicated duration. The protein extraction was detected by immunoblot analysis. (E–F) DHS induced Nrf2 nuclear translocation. For E, cells were exposed to 4 μM DHS or 5 μM SF for 8 h followed by indirect fluorescence staining. The scale bar was 20 μm. For F, cells were treated with 4 μM DHS or 5 μM SF for 8 h followed by nuclear and cytoplasmic protein extraction. Results are expressed as mean ± SD (n = 3). $*p < 0\ 05$ treated versus control.

protein-protein interaction (PPI). To test the function of DHS on it, Beas-2B cells transfected with Nrf2 and Keap1 plasmids, were treated with DHS, and the cell lysates were immunoprecipitated with anti-Keap1 antibody and blotted with anti-Nrf2 and anti-Keap1 bodies. As observed in Fig. 4C, DHS treatment increased the Nrf2 protein level, and has no effect on the Keap1 protein expression. Immunoprecipitation showed that the ratio of Nrf2 to Keap1 decreased with the DHS treatment, suggesting that DHS interrupted the Nrf2-Keap1 PPI (Fig. 4C). Since Keap1 contains many cysteine residues which bears high-reactive sulfhydryl groups, Nrf2 activators can react with these cysteines by covalent bonds, produce an alteration of Keap1 conformation, and promote the release of Nrf2 from Keap1. Among

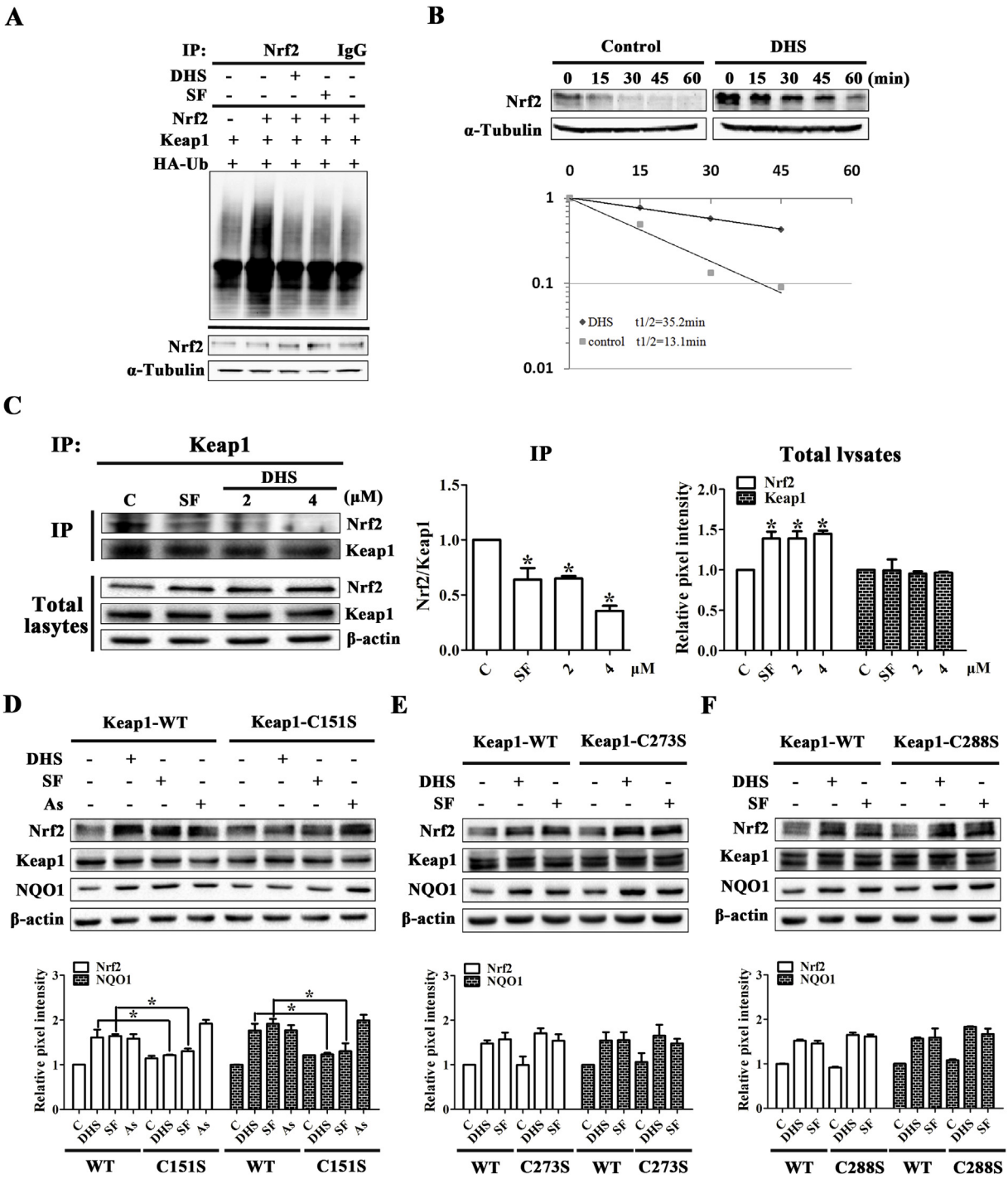

Fig. 4. DHS blocks Nrf2 ubiquitylation and activates Nrf2 in a Keap1-Cys151-dependent manner. (A) DHS inhibited Nrf2 ubiquitination. The Nrf2, Keap1, hemagglutinin (HA)-ubiquitin, and vector plasmids were cotransfected into cells. The transfected cells were exposed to 4 μM DHS or 2 μM positive control drug SF, together with MG132 (10 μM) for 6 h, and then collected cells and performed immunoblot analysis and immunoprecipitation analysis. (B) DHS extended the half-life of Nrf2. Beas-2B cells were pretreated with or without 4 μM DHS for 8 h, and then exposed to 50 μM CHX. Protein lysates were collected at 0, 10, 20, 30, 40 min, and were subjected to immunoblot analysis. (C) DHS interrupted interaction between Keap1 and Nrf2. Beas-2B cells transfected with Nrf2 and Keap1 plasmids were treated with 2 μM and 4 μM DHS or 2 μM SF for 12 h, together with MG132 (10 μM) for 6 h, and then collected cells and performed immunoblot analysis and immunoprecipitation analysis. (D–F) DHS increased level of Nrf2 protein in a Keap1-Cys151-dependent manner. The Keap1-siRNA, together with wild-type Keap1 (Keap1-WT) or mutated Keap1 (Keap1-C151S for D, Keap1-C273S for E, and Keap1-C288S for F) plasmids were cotransfected into Beas-2B cells, and then the cells were treated with 4 μM DHS, 2.5 μM SF or 10 μM As(III) for 18 h. Results are expressed as mean ± SD (n = 3). For C, ∗p < 0 05 treated vs. control. For D-F, ∗p < 0 05 Keap1-mutated vs. Keap1-WT.

these cysteine residues, Cys151, Cys273 and Cys288 play a vital role for Keap1-dependent activation of Nrf2. Herein, we investigated the potential reaction between DHS and these three high-reactive cysteines. Cells were transfected with Keap1-siRNA to silence endogenous Keap1 and displaced with wild-type Keap1 (Keap1-WT) or mutated Keap1 (Keap1-C151S, Keap1-C273S, and Keap1-C288S) by transfection. As shown in Fig. 4D–F, similar to SF, DHS upregulated the protein level of Nrf2 in the cells transfected with Keap1-WT, Keap1-C273S, and Keap1-

C288S. However, increased level of Nrf2 protein by DHS or SF treatments was prevented in the cells transfected with Keap1-C151S. Collectively, these data implies that DHS activates Nrf2 through blocking Nrf2 ubiquitylation and reacting with Cys151 cysteine in Keap1 protein.

3.5. DHS inhibits LPS-stimulated inflammatory response in RAW 264.7 cells

The potential inhibitory effect of DHS against inflammatory response was investigated using a LPS-stimulated inflammatory model in RAW 264.7 macrophages. The proinflammatory mediators (e.g. NO, IL-6, IL-1β, TNF-α, iNOS, MMP-9 and COX-2) which are involved in the inflammatory response of COPD, have been determined. DHS dose-dependently inhibited LPS-induced overproduction of NO from the dose of 0.2 μM, and no cytotoxicity was observed below the doses of 3.12 μM (Fig. 5A). The doses ≤2 μM were selected for the subsequent bioassay. Immunoblot analysis indicated that DHS suppressed LPS-stimulated overexpression of COX-2 and iNOS (Fig. 5B). As depicted in Fig. 5C–E, DHS reverted LPS-stimulated upregulations of IL-6, IL-1β, and TNF-α,

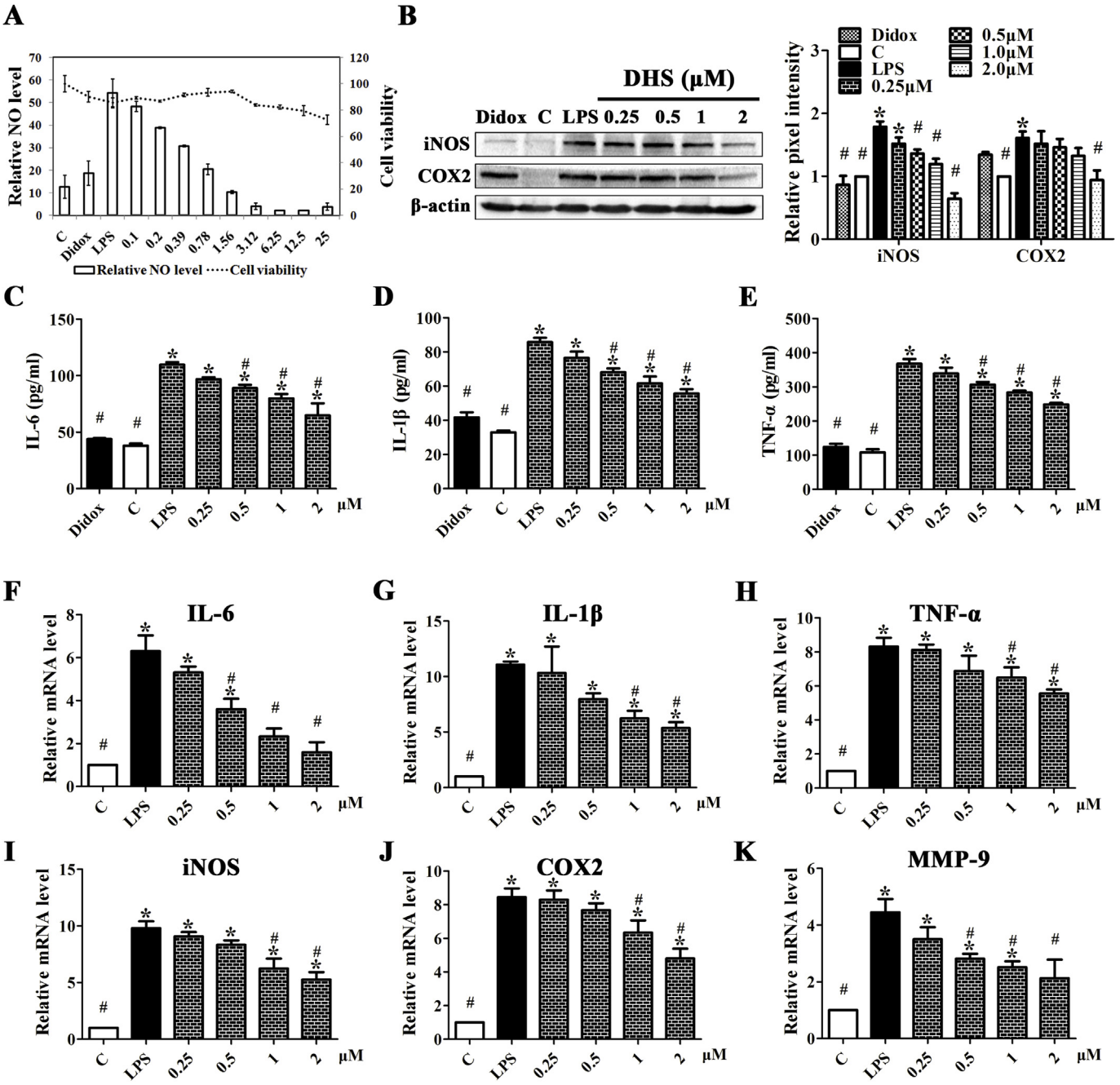

Fig. 5. DHS inhibits LPS-stimulated inflammatory response in RAW 264.7 cells. (A) DHS inhibited LPS-induced overproduction of NO. RAW cells were exposed to indicated concentrations of DHS or Didox (100 μM), together with LPS (1 μg/mL) for 24 h. NO levels in supernatant were analyzed using Griess reagent. (B) DHS reverted LPS-stimulated activation of iNOS and COX-2 in the protein levels. Cells were pretreated with specified doses of DHS for 1 h, followed by cotreatment with DHS and LPS (1 μg/mL) for additional 16 h. (C–E) DHS reverted LPS-stimulated upregulations of IL-6, IL-1β, and TNF-α. The contents of cytokine in the culture media were measured with ELISA kits. (F-K) DHS blocked LPS-stimulated increase of proinflammatory mediators in mRNA levels. RAW cells were pretreated with varying concentrations of DHS for 1 h, followed by cotreatment with DHS and LPS (1 μg/mL) for additional 16 h. The mRNA contents were examined with RT-PCR. Results are expressed as mean ± SD (n = 3). $*p < 0\ 05$ treated versus control; $\#p < 0.05$ treated versus LPS-treated alone.

which were detected by ELISA. Furthermore, we measured the mRNA levels of IL-6, IL-1β, TNF-α, iNOS, MMP-9 and COX-2 in response to LPS stimulation in the presence or absence of DHS by qRT-PCR. LPS-stimulated increases of these proinflammatory mediators have been dose-dependently blocked (Fig. 5F–K). Therefore, these results definitely support that DHS inhibits LPS-induced inflammatory response in RAW264.7 cells *in vitro*.

3.6. DHS inhibits LPS-stimulated activation of NF-κB in RAW 264.7 cells

Since NF-κB is a key regulator of inflammatory response and involved in the regulation of proinflammatory mediators (e.g. IL-6, IL-1β, TNF-α, iNOS, MMP-9 and COX-2), we determined the effect of DHS on NF-κB pathway. DHS inhibited LPS-stimulated NF-κB transcription in the dual luciferase assay (Fig. S3). Exposure of cell to LPS gave rise to upregulations of NF-κB p65 and P-p65 protein levels, and a decrease of IκBα protein level (Fig. 6A). However, the protein levels of NF-κB p65 and P-p65 decreased in a dose-dependent manner when cells were treated by DHS (Fig. 6A). As expected, the protein level of LPS-stimulated decrease of IκBα was dose-dependently reverted by DHS. When cells are exposed to stimuli (e.g. LPS), NF-κB p65 escapes from IκB-α, translocates to the nucleus, and activates the inflammation-related genes. As depicted in Fig. 6B, NF-κB p65 subunit accumulated in the nuclear after exposure to LPS, while DHS suppressed the process of its nuclear translocation, which was further confirmed by measuring the protein level of NF-κB p65 in nucleus and cytoplasm (Fig. 6C). Thus, these results indicate that DHS is able to inhibit NF-κB-mediated inflammatory response in RAW 264.7 cells.

3.7. DHS alleviates CS-induced pulmonary pathological impairment and fibrosis

To investigate the potential prevention and therapy of DHS against COPD, a CS-induced pulmonary impairment mice model has been established. During sixteen weeks' exposure, the body weights and the food intake of mice in control group are higher than that of mice exposed to CS, and no significant difference were observed in the mice cotreated with CS and DHS, tBHQ, and Dex (Fig. S4). After sixteen weeks' exposure, the lung tissues were collected and subjected to analysis (Fig. 7A). HE and PAS staining indicated that the lungs in mice exposed to CS alone demonstrated typical features for pathological alterations and inflammatory response, including thickening of the alveolar septa, proliferation of fibroblasts, hyperplasia of pneumocytes, distinct infiltration of leukocytes, and goblet cell hyperplasia in peribronchial and perivascular areas (Fig. 7B–C). Similar with the positive control tBHQ and Dex, DHS treatment evidently attenuated CS-induced inflammatory response and pathological changes (Fig. 7B–C). Masson staining indicated that CS-induced pulmonary fibrosis could be alleviated by DHS treatment (Fig. 7D). Activation of TGF-β1 is a key mechanism for the lung fibrosis, and we determined the content of TGF-β1 in lung tissues using IHC staining and ELISA. Exposure to CS led to a significant increase of TGF-β1 in the lung tissue. However, CS-induced upregulation of TGF-β1 has been evidently inhibited by DHS, tBHQ, and Dex treatments (Fig. 7E–F). Therefore, these results indicate that DHS alleviates CS-induced pulmonary pathological impairment and fibrosis.

3.8. DHS relieves CS-induced pulmonary oxidative insults via activation of Nrf2

Activation of Nrf2-mediated antioxidant response and oxidative insults in the lung tissue were determined to verify the beneficial effect of DHS against CS-induced pulmonary oxidative damages. The protein level of Nrf2 and its target gene NQO1 slightly increased after exposure to CS, suggesting that Nrf2-mediated antioxidant response was induced by oxidants from CS and CS-stimulated inflammatory cells (Fig. 8A). Consistent with the results of study *in vitro* (Fig. 3C), treatment with DHS markedly upregulated the protein expressions of Nrf2 and NQO1 as measured by immunoblot analysis (Fig. 8A) and immunohistochemistry (IHC) (Fig. 8B). Accordingly, DHS treatment enhanced production of endogenous antioxidant GSH (Fig. 8C). Importantly, DHS significantly reduced CS-induced oxidative damage in the lung, as measured by the levels of MDA in the lung tissue (Fig. 8D). Next, ELISA and IHC analysis for 8-oxo-dG in lung were performed to evaluate CS-induced oxidative DNA damage. As depicted in Fig. 8E and F, CS-induced enhancement of 8-oxo-dG content and its staining were

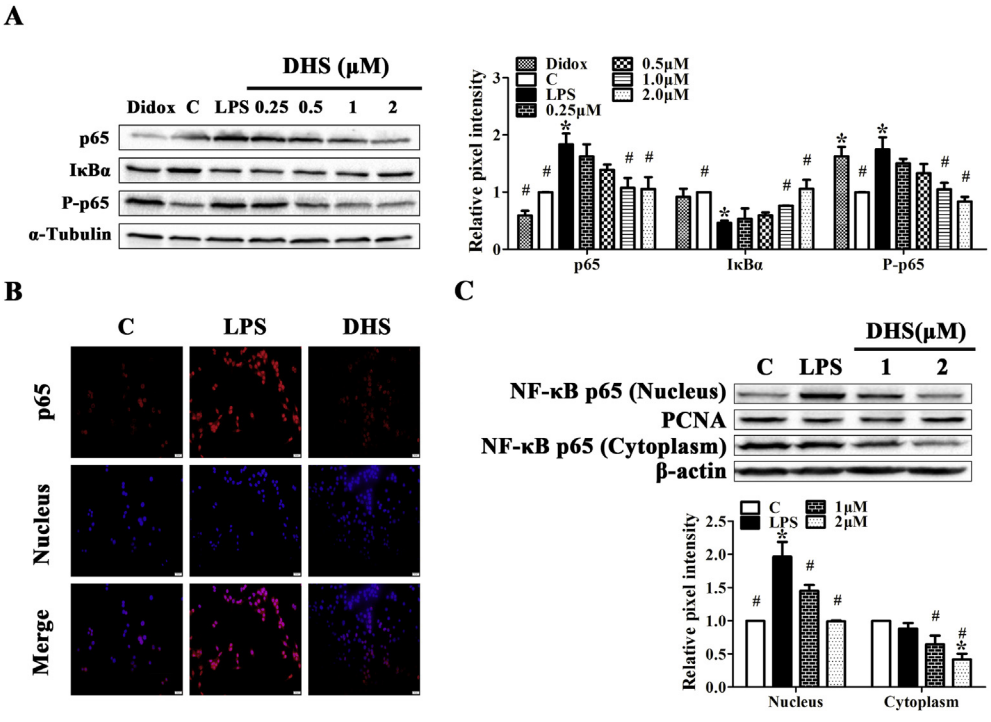

Fig. 6. DHS inhibits NF-κB-mediated inflammatory response in RAW 264.7 cells. (A) DHS reverted LPS-stimulated activation of NF-κB p65, IκBα and P-p65 in the protein levels. Cells were pretreated with specified doses of DHS for 1 h, and followed by co-treatment with DHS and LPS (1 μg/mL) for additional 3 h. (B-C) DHS suppressed the LPS-stimulated NF-κB p65 nuclear translocation. Cells were exposed to 2 μM DHS for 1 h, followed by cotreatment with DHS and LPS (1 μg/mL) for additional 3 h, and then were subjected to fluorescence staining (B) and nuclear and cytoplasmic protein extraction (C). Results are expressed as mean ± SD (n = 3). $*p < 0\ 05$ treated versus control; $\#p < 0.05$ treated versus LPS-treated alone.

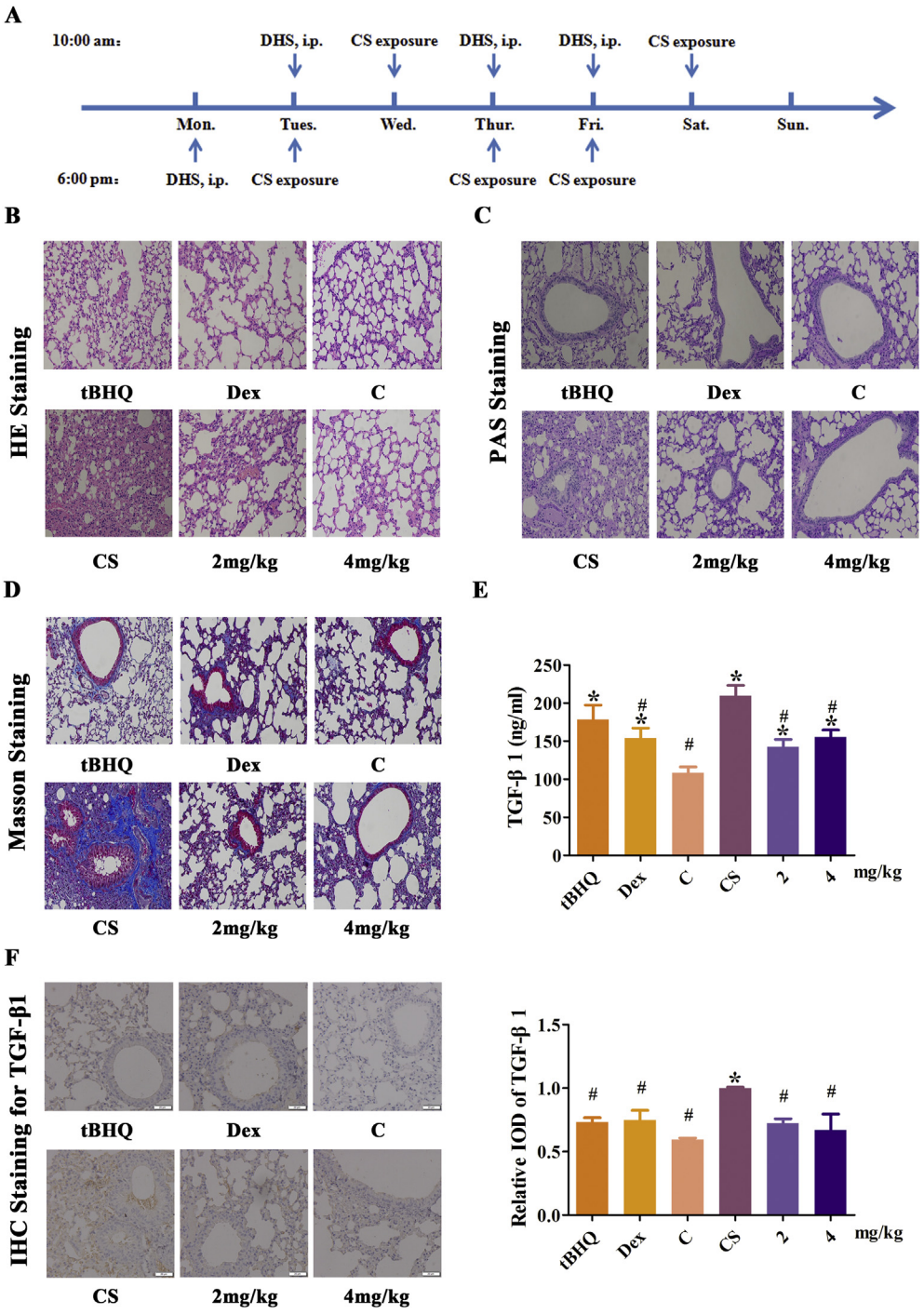

Fig. 7. DHS alleviates CS-induced pulmonary physiological impairment and fibrosis. (A) Schematic of the experimental procedures of injection and CS exposure in a week. (B-C) DHS alleviated CS-induced pulmonary physiological impairment. Lung tissue sections were stained with H&E for B or PAS for C. The images of sections were observed under 200X magnification. (D) DHS alleviated CS-induced pulmonary fibrosis. Lung tissue sections were stained with Masson's trichrome, and then the images of sections were observed under 200X magnification. (E–F) DHS inhibited CS-induced upregulation of TGF-β1. The content of TGF-β1 in lung tissues was determined using ELISA (E) and IHC staining (F). Results are expressed as mean ± SD (n = 3). $*p < 0\ 05$ treated versus control; $\#p < 0.05$ treated versus CS.

significantly inhibited by DHS treatment. Collectively, these data imply that DHS activates Nrf2-mediated antioxidant response, and relieves CS-induced pulmonary oxidative insults *in vivo*.

3.9. DHS attenuates CS-induced pulmonary inflammation via inhibition of NF-κB

Inhibition of NF-κB-mediated inflammatory response in the lung tissue was tested to confirm the beneficial effect of DHS against CS-induced pulmonary inflammation. Immunoblot analysis indicated that CS-induced upregulation of P-NF-κB p65 protein expression could be evidently reverted by DHS, tBHQ, and Dex (Fig. 9A). As expected, this result was further confirmed by IHC analysis of NF-κB p65 in lung tissue (Fig. 9B). Next, we determined the levels of proinflammatory mediators, including TNF-α, IL-6, and IL-1β, in BALF (Fig. 9C–E) and serum (Fig. 9F–H) using ELISA. Mice receiving CS exposure alone had a greater degree of inflammatory response as shown by the significantly increased levels of TNF-α, IL-6, and IL-1β in BALF and serum (Fig. 9C–H). Importantly, DHS administration alleviated CS-induced increases of these three pro-inflammatory mediators. Collectively, these data suggest that DHS attenuates CS-induced pulmonary inflammatory response via inhibition of NF-κB.

4. Discussion

Interest in resveratrol has been kept and renewed for a long time,

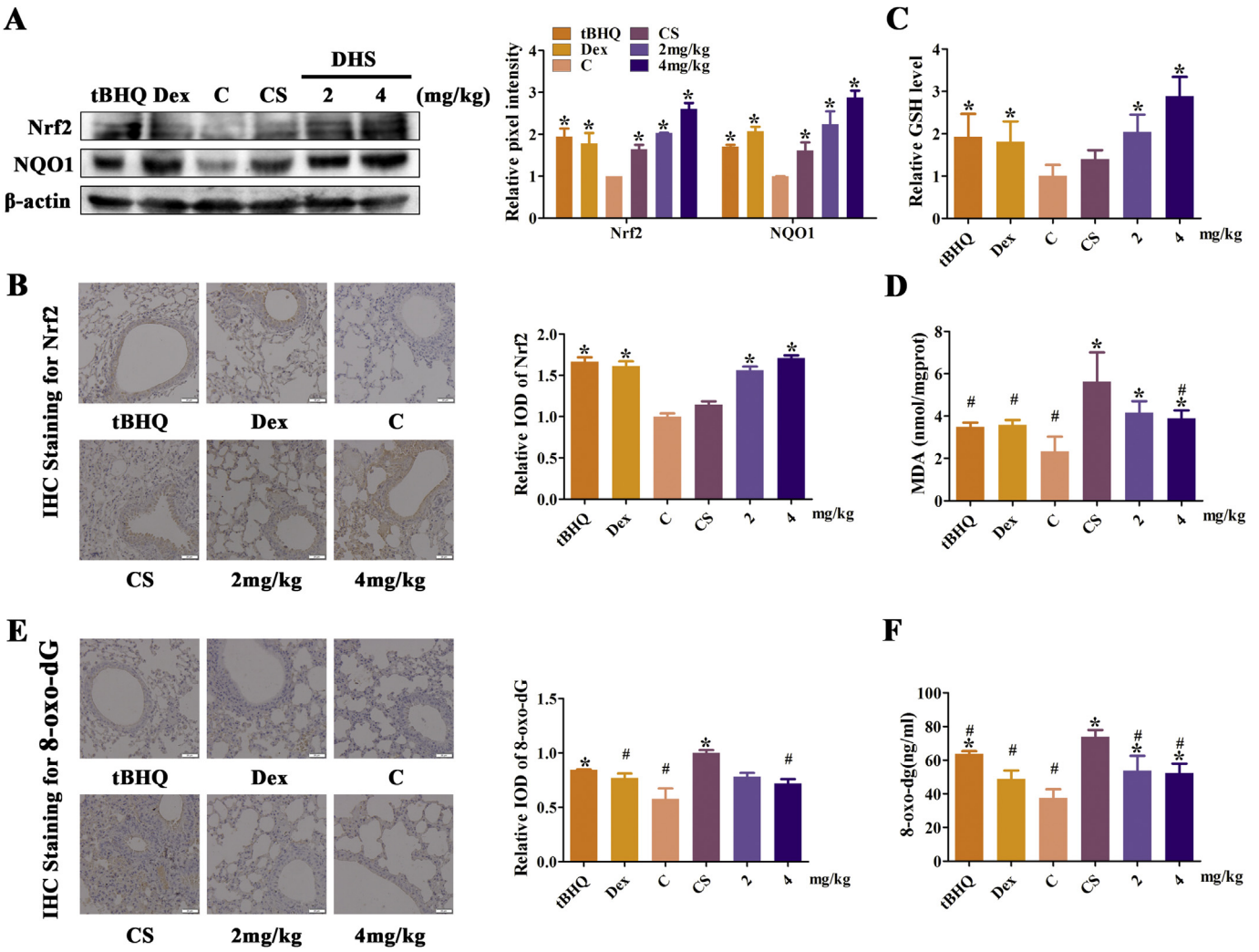

Fig. 8. DHS relieves CS-induced oxidative insults via activation of Nrf2. (A–B) DHS upregulated the levels of Nrf2 and NQO1 in the lung tissue. For A, the protein extraction was analyzed by immunoblot analysis. For B, the expression of Nrf2 in lung tissue was determined using IHC staining. (C) DHS enhanced production of reduced GSH. The contents of GSH in the lung homogenate were measured by reduced GSH kits. (D) DHS reverted CS-induced increase of MDA. The contents of MDA in the lung homogenate were measured by MDA kits. (E–F) DHS inhibited CS-induced enhancement of 8-oxo-dG. The content of 8-oxo-dG in lung tissues was determined using IHC staining (E) and ELISA (F). Results are expressed as mean ± SD (n = 3). $*p < 0\ 05$ treated versus control; $\#p < 0.05$ treated versus CS.

since its diverse biological functions of chemoprevention, cardioprotection, prolongation of lifespans of lower organism, and so on [23,24]. A growing body of evidence *in vivo* demonstrated the beneficial effects of resveratrol against human diseases, and some clinical trials have been performed for oral resveratrol against cancer [15]. However, its poor bioavailability definitely limited its medical application. For instance, the effective doses commonly used were 10–50 μM for different cell-based assays [25], 5–100 mg per kg for various mice models [26,27], and 7.5 g per day for the clinical trial [15]. Therefore, plenty of researches have been performed to discovering resveratrol analogues with potent efficiency and good bioavailability, and accordingly to increase its feasibility to be developed as a clinical drug. A battery of literature reported that resveratrol exerted endothelium protective [18], cardioprotective [28], anti-inflammatory [19], and antioxidant properties [29], because of its capability of inducing Nrf2 signaling pathway. Herein, we verified that resveratrol is a weak Nrf2 inducer (Fig. S1). To improve its capability of activating Nrf2, a series of resveratrol analogues were prepared and subjected to biological investigation. DHS is a stilbene-type molecule with anti-tumor effect verified by previous researches, and has been isolated from the bark of *Yucca periculosa* [30–32]. In the present research, the Nrf2 inducing effect of DHS was firstly identified. Similar to its parent compound resveratrol, DHS possesses a poor bioavailability, which could be evidently improved by pharmaceutical techniques (e.g. solubilization via adding hydroxypropyl-β-cyclodextrin) [33]. Importantly, DHS was more potent than the well-known Nrf2 activator SF, and displayed an approximately > 10-fold increase of Nrf2-inducing effect than that of resveratrol, with a minimum effective dose of 130 nM (Fig. 1A, C, 3A-B, S1 and S2). High potency of DHS might improve its opportunity to become a clinically used drug. Therefore, our resveratrol-based chemical modification leads to the finding a potent Nrf2 activator DHS, which might be a promising agent against human diseases.

There is a driving need to develop preventive and therapeutic agent against COPD targeting its pathological process. Oxidative stress, inflammatory response, protease-antiprotease imbalance and their interaction have been found to be related to the onset and progression of COPD [34]. Our experiments *in vitro* indicated that DHS enhanced antioxidant capacity and protected cells against toxicant-induced oxidative stress (Fig. 2). Nrf2 is released from Keap1 and translocates into the nucleus, and activatescytoprotective genes in response to oxidants, toxicants or inducers [5]. We have observed that DHS promoted Nrf2 nuclear translocation (Fig. 3E and F), activated Nrf2-regulated defensive response via suppressing its Keap1-mediated Nrf2 ubiquitination and degradation of Nrf2, and thus enhancing Nrf2 protein stabilization

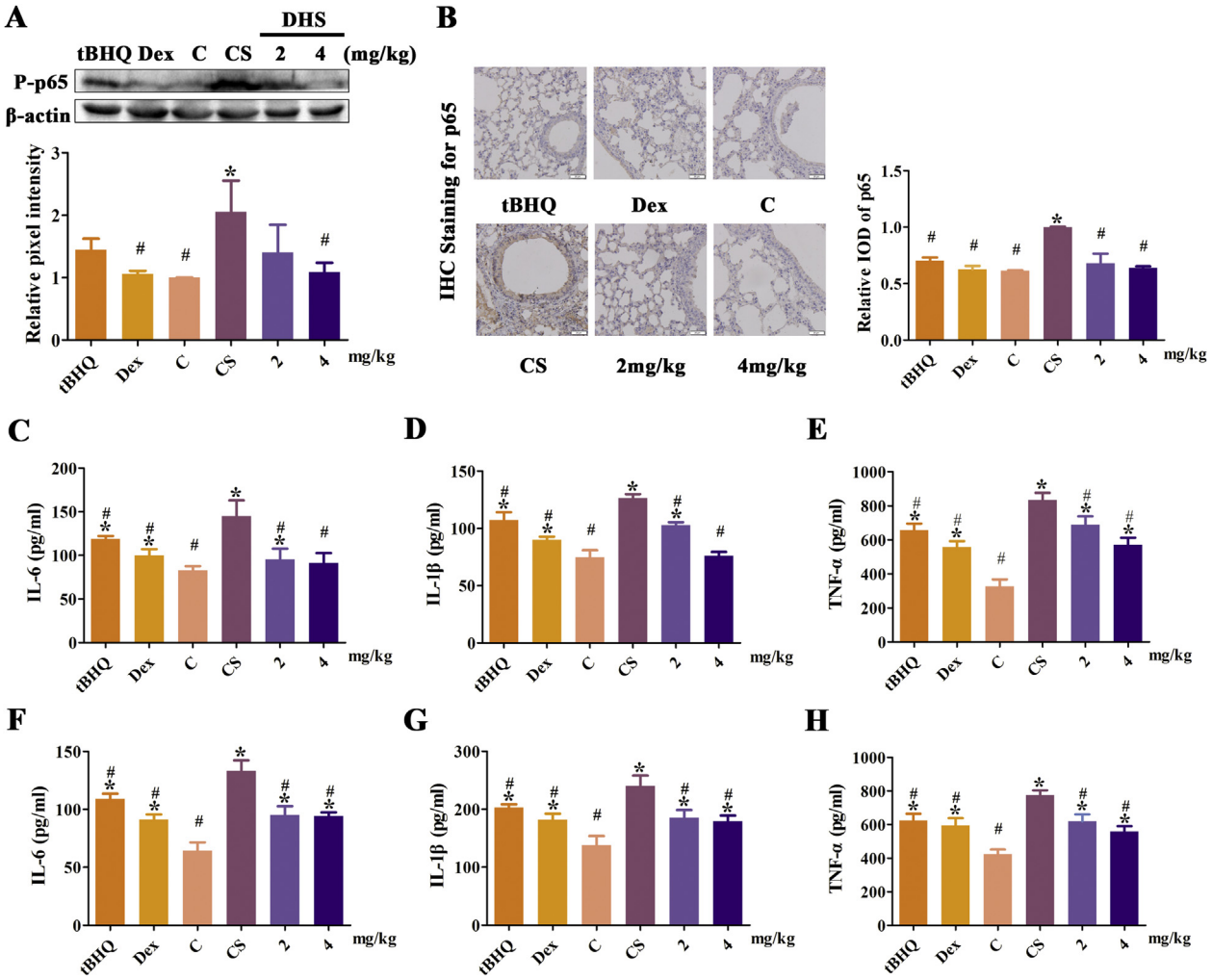

Fig. 9. DHS attenuates CS-induced inflammation via inhibition of NF-κB. (A–B) DHS blocked CS-induced upregulation of NF-κB p65 and P-p65 in the lung tissue. For A, the protein extraction was analyzed by immunoblot analysis. For B, The expression of NF-κB p65 in lung tissue was determined using IHC staining. (C-H) DHS alleviated CS-induced increases of IL-6, IL-1β, and TNF-α. The levels of proinflammatory mediators in BALF (C–E) and serum (F-H) were measured by ELISA kits. Results are expressed as mean ± SD (n = 3). $*p < 0.05$ treated versus control; $\#p < 0.05$ treated versus CS.

(Fig. 4A and B). Modification of Keap1 reactive cysteine residues is an important mechanism for Nrf2 activation, and Cys151, Cys273, and Cys288 have been found to be essential for regulating Nrf2 degradation [35–38], implying that these cysteines are sensor sites for Nrf2 activators. Similar to the induction of Nrf2 by SF is highly dependent on Cys151 of Keap1 [39], we have identified Cys151, but not Cys273 and Cys288 as a site of Keap1 DHS reaction (Fig. 4D–F). In addition, DHS evidently inhibited LPS-stimulated inflammatory response *in vitro*, and the redox-sensitive NF-κB and pro-inflammatory mediators (e.g. IL-6, IL-1β, TNF-α, iNOS, MMP-9 and COX-2), that were involved in the pathological process of COPD, have been suppressed in mRNA or protein levels (Figs. 5 and 6). Our observations in bioassay *in vitro* verified that DHS was a molecule with potent inhibitions against oxidative stress and inflammatory response. Given the vial roles of oxidative stress and inflammatory response in onset and progression of COPD, DHS deserves to be sufficiently investigated using a COPD model *in vivo*.

Cigarette smoke (CS) contains high contents of free radicals and oxidants, and is through to be the predominant cause of COPD and lung cancer worldwide [1]. Hence, we used a CS-induced pulmonary impairment mice model to evaluate the protective effect of DHS [40]. It has been well documented that CS exposure causes damage of epithelial cells, stimulates productions of pro-inflammatory mediators, and induces infiltration and activation of neutrophils and macrophages [41,42]. These two types of inflammatory cells can release endogenous ROS and reactive nitrogen species (RNS) to aggravate oxidant burden, and generate excessive elastase and metalloproteinases (MMPs) to facilitate destruction of alveolar walls. In our established CS-induced pulmonary impairment model group, excessive respiratory oxidative stress, and inflammatory response verified by the increased levels of oxidant biomarkers MDA and 8-oxo-dG, as well as upregulated expressions of pro-inflammatory mediators (e.g. IL-6, IL-1β, TNF-α), have been observed (Fig. 8D–F and 9C-H). Meanwhile, we have also detected the respiratory pathological alterations induced by CS, exemplified by infiltration of leukocytes, and proliferation of fibroblasts (Fig. 7B–D). DHS at concentrations of 2 and 4 mg/kg significantly alleviated CS-induced pathological changes (Fig. 7B–D), suggesting that DHS was a potential agent for the prevention of pulmonary impairment.

The protein level of Nrf2 and its target gene NQO1 slightly increased after exposure to CS (Fig. 8A–B). Compared with the control group, no evident changes of the intracellular antioxidant GSH level in CS-treated group has been detected (Fig. 8C). It is rational that Nrf2-mediated antioxidant response is induced to counteract the insults caused by exposure to CS. However, CS-induced upregulation of Nrf2-mediated antioxidant response could not efficiently prevent the impairment because of low basal level of Nrf2 in the lung. When the mice were administrated with DHS, there was a sharp increases of Nrf2, NQO1, and GSH (Fig. 8A–C), which significantly attenuated CS-induced oxidative stress and lung impairment. It has been observed that CS

exposure gave rise to decreases of body weight and food consumption, however, induction of Nrf2 by DHS did not alleviate the loss of body weight and food consumption (Fig. S4). Besides these tested proteins and enzymes, combined activation of the Nrf2-mediated defensive system, covering intracellular antioxidant enzymes and phase II detoxifying enzymes (e.g. GCLM, NOQ1, HO-1), and many other cytoprotective proteins, may contribute to the DHS-mediated protection against CS-stimulated pulmonary impairment in mice model.

Literature reported that CS was a potent stimulator of NF-κB in the lung, and stimulated inflammatory response by NF-κB-dependent production of inflammatory mediators [43]. These inflammatory mediators are involved in CS-induced ongoing inflammatory response, and lead to parenchymal tissue destruction (resulting in emphysema) and disrupted normal repair and defense mechanisms (resulting in small airway fibrosis) [1]. When NF-κB is activated by CS exposure, IL-6 and IL-1β is overproduced by innate immune system cells (e.g. macrophages, neutrophils, and B lymphocyte), and significantly increased compared with non-smokers [44]. TNF-α level is raised in sputum of COPD patient, and a positive correlation between the level of TNF-α and the severity of COPD has been observed [45]. TNF-α enhances inflammatory response and induces IL-8 and other chemokines in airway cells. MMP-9 is a protease, and overexpressed by alveolar macrophages in the COPD patients [46]. It is able to damage connective tissue in the lung parenchyma to give emphysema. The potent fibrosis inducer of TGF-β1 is highly expressed in epithelium cells and macrophages of small airways in COPD patient [47]. Furthermore, TGF-β1 can stimulate MMP-9, and MMP-9 regulates proteolysis of TGF-β1 binding protein, which could be a mechanism for physiological release of TGF-β1 [48]. Increased levels of MMP-9 and TGF-β1 form a positive cycle and aggravate the emphysema and fibrosis. Given their biological functions, inhibitions of these proinflammatory mediators have been regarded to be effective strategy for the therapy of COPD [13]. Herein, our results indicate that DHS inhibits these inflammatory mediators, covering IL-6, IL-1β, TNF-α, MMP-9, and TGF-β1, in the bioassay *in vitro* or *in vivo*.

Besides regulation on oxidative stress, Nrf2 is able to suppress the inflammatory response. Nrf2-deficiency gives rise to an exacerbation of inflammation-related diseases verified by the experiments *in vivo* [8,49,50]. It is well-recognized that Nrf2-mediated upregulation of antioxidant enzymes, and increased ability of eliminating ROS is the predominant molecular mechanism of Nrf2-associated anti-inflammatory property [51–53]. Therefore, there is a negative regulation of Nrf2 on inflammatory mediators in a ROS-independent manner. More interestingly, a recent study indicated that Nrf2 suppressed expressions of proinflammatory cytokine genes (e.g. IL-6 and IL-1β) through the ROS-independent transcriptional inhibition [54]. Nrf2 can bind to the proximity of proinflammatory genes and suppress their RNA polymerase II recruitment. Based on these findings, relief of CS-induced damage might be also related to the inhibitions of Nrf2 on the expressions of IL-6, IL-1β, TNF-α, iNOS, MMP-9, and COX-2.

Taken together, our findings indicate that the synthetic resveratrol analogue DHS potently inhibits oxidative stress through activating Nrf2 pathway. Furthermore, DHS effectively suppresses inflammatory response via inhibiting NF-κB. More importantly, an *in vivo* study demonstrates the feasibility of preventing CS-induced pulmonary impairment by administration of DHS. On the basis of these promising results, a detailed pharmacokinetic and pharmacodynamic investigation of DHS should be performed to evaluate its bioavailability and druggability.

Declaration of Competing interest

The Author(s) declare(s) that they have no conflicts of interest to disclose.

Acknowledgments

This work was supported by National Natural Science Foundation of China of China (Nos. 81874341, 31100607, and 81673558), the key research and development program of Shandong province (No. 2018GSF118085), and Young Scholars Program of Shandong University (Nos. 2015WLJH50 and 2018WLJH93).

Appendix A. Supplementary data

Supplementary data to this article can be found online at https://doi.org/10.1016/j.freeradbiomed.2019.11.026.

References

[1] J. Vestbo, S.S. Hurd, A.G. Agusti, P.W. Jones, C. Vogelmeier, A. Anzueto, P.J. Barnes, L.M. Fabbri, F.J. Martinez, M. Nishimura, R.A. Stockley, D.D. Sin, R. Rodriguez-Roisin, Global strategy for the diagnosis, management, and prevention of chronic obstructive pulmonary disease GOLD executive summary, Am. J. Respir. Crit. Care Med. 187 (4) (2013) 347–365, https://doi.org/10.1164/rccm.201204-0596PP.

[2] G. Gloire, S. Legrand-Poels, J. Piette, NF-kappa B activation by reactive oxygen species: fifteen years later, Biochem. Pharmacol. 72 (11) (2006) 1493–1505, https://doi.org/10.1016/j.bcp.2006.04.011.

[3] T. Dey, P. Dutta, P. Manna, J. Kalita, H.P.D. Boruah, A.K. Buragohain, B. Unni, D. Ozah, M.K. Goswami, R.K. Kotokey, Cigarette smoke compounds induce cellular redox imbalance, activate NF-kappa B, and increase TNF-alpha/CRP secretion: a possible pathway in the pathogenesis of COPD, Toxicol. Res. 5 (3) (2016) 895–904, https://doi.org/10.1039/c5tx00477b.

[4] V. Austin, P.J. Crack, S. Bozinovski, A.A. Miller, R. Vlahos, COPD and stroke: are systemic inflammation and oxidative stress the missing links? Clin. Sci. 130 (13) (2016) 1039–1050, https://doi.org/10.1042/CS20160043.

[5] M.C. Jaramillo, D.D. Zhang, The emerging role of the Nrf2-Keap1 signaling pathway in cancer, Genes Dev. 27 (20) (2013) 2179–2191, https://doi.org/10.1101/gad.225680.113.

[6] A. Lau, N.F. Villeneuve, Z. Sun, P.K. Wong, D.D. Zhang, Dual roles of Nrf2 in cancer, Pharmacol. Res. 58 (5–6) (2008) 262–270, https://doi.org/10.1016/j.phrs.2008.09.003.

[7] M.J. Morgan, Z.G. Liu, Crosstalk of reactive oxygen species and NF-kappa B signaling, Cell Res. 21 (1) (2011) 103–115, https://doi.org/10.1038/cr.2010.178.

[8] T. Iizuka, Y. Ishii, K. Itoh, T. Kiwamoto, T. Kimura, Y. Matsuno, Y. Morishima, A.E. Hegab, S. Homma, A. Nomura, T. Sakamoto, M. Shimura, A. Yoshida, M. Yamamoto, K. Sekizawa, Nrf2-deficient mice are highly susceptible to cigarette smoke-induced emphysema, Genes Cells 10 (12) (2005) 1113–1125, https://doi.org/10.1111/j.1365-2443.2005.00905.x.

[9] M. Suzuki, T. Betsuyaku, Y. Ito, K. Nagai, Y. Nasuhara, K. Kaga, S. Kondo, M. Nishimura, Down-regulated NF-E2-Related factor 2 in pulmonary macrophages of aged smokers and patients with chronic obstructive pulmonary disease, Am. J. Respir. Cell Mol. Biol. 39 (6) (2008) 673–682, https://doi.org/10.1165/rcmb.2007-0424OC.

[10] A. Di Stefano, G. Caramori, T. Oates, A. Capelli, M. Lusuardi, I. Gnemmi, F. Ioli, K.F. Chung, C.F. Donner, P.J. Barnes, I.M. Adcock, Increased expression of nuclear factor-kappa B in bronchial biopsies from smokers and patients with COPD, Eur. Respir. J. 20 (3) (2002) 556–563, https://doi.org/10.1183/09031936.02.00272002.

[11] G. Caramori, M. Romagnoli, P. Casolari, C. Bellettato, G. Casoni, P. Boschetto, K.F. Chung, P.J. Barnes, I.M. Adcock, A. Ciaccia, L.M. Fabbri, A. Papi, Nuclear localisation of p65 in sputum macrophages but not in sputum neutrophils during COPD exacerbations, Thorax 58 (4) (2003) 348–351, https://doi.org/10.1136/thorax.58.4.348.

[12] A. Boutten, D. Goven, E. Artaud-Macari, J. Boczkowski, M. Bonay, NRF2 targeting: a promising therapeutic strategy in chronic obstructive pulmonary disease, Trends Mol. Med. 17 (7) (2011) 363–371, https://doi.org/10.1016/j.molmed.2011.02.006.

[13] P.J. Barnes, T.T. Hansel, Prospects for new drugs for chronic obstructive pulmonary disease, Lancet 364 (9438) (2004) 985–996, https://doi.org/10.1016/S0140-6736(04)17025-6.

[14] C.A. de la Lastra, I. Villegas, Resveratrol as an anti-inflammatory and anti-aging agent: mechanisms and clinical implications, Mol. Nutr. Food Res. 49 (5) (2005) 405–430, https://doi.org/10.1002/mnfr.200500022.

[15] J.A. Baur, D.A. Sinclair, Therapeutic potential of resveratrol: the in vivo evidence, Nat. Rev. Drug Discov. 5 (6) (2006) 493–506, https://doi.org/10.1038/nrd2060.

[16] D. Delmas, B. Jannin, N. Latruffe, Resveratrol: preventing properties against vascular alterations and ageing, Mol. Nutr. Food Res. 49 (5) (2005) 377–395, https://doi.org/10.1002/mnfr.200400098.

[17] K. Szkudelska, T. Szkudelski, Resveratrol, obesity and diabetes, Eur. J. Pharmacol. 635 (1–3) (2010) 1–8, https://doi.org/10.1016/j.ejphar.2010.02.054.

[18] Z. Ungvari, Z. Bagi, A. Feher, F.A. Recchia, W.E. Sonntag, K. Pearson, R. de Cabo, A. Csiszar, Resveratrol confers endothelial protection via activation of the antioxidant transcription factor Nrf2, Am. J. Physiol. Heart Circ. Physiol. 299 (1) (2010) H18–H24, https://doi.org/10.1152/ajpheart.00260.2010.

[19] P. Palsamy, S. Subramanian, Resveratrol protects diabetic kidney by attenuating hyperglycemia-mediated oxidative stress and renal inflammatory cytokines via Nrf2-Keap1 signaling, Biochim. Biophys. Acta (BBA) - Mol. Basis Dis. 1812 (7) (2011) 719–731, https://doi.org/10.1016/j.bbadis.2011.03.008.

[20] N. Tamaki, R.C. Orihuela-Campos, Y. Inagaki, M. Fukui, T. Nagata, H.O. Ito, Resveratrol improves oxidative stress and prevents the progression of periodontitis via the activation of the Sirtl/AMPK and the Nrf2/antioxidant defense pathways in a rat periodontitis model, Free Radic. Biol. Med. 75 (2014) 222–229, https://doi.org/10.1016/j.freeradbiomed.2014.07.034.

[21] A. Kode, S. Rajendrasozhan, S. Caito, S.R. Yang, I.L. Megson, I. Rahman, Resveratrol induces glutathione synthesis by activation of Nrf2 and protects against cigarette smoke-mediated oxidative stress in human lung epithelial cells, Am. J. Physiol. Lung Cell Mol. Physiol. 294 (3) (2008) L478–L488, https://doi.org/10.1152/ajplung.00361.2007.

[22] K. Jomova, Z. Jenisova, M. Feszterova, S. Baros, J. Liska, D. Hudecova, C.J. Rhodes, M. Valko, Arsenic: toxicity, oxidative stress and human disease, J. Appl. Toxicol. 31 (2) (2011) 95–107, https://doi.org/10.1002/jat.1649.

[23] M.S. Jang, E.N. Cai, G.O. Udeani, K.V. Slowing, C.F. Thomas, C.W.W. Beecher, H.H.S. Fong, N.R. Farnsworth, A.D. Kinghorn, R.G. Mehta, R.C. Moon, J.M. Pezzuto, Cancer chemopreventive activity of resveratrol, a natural product derived from grapes, Science 275 (5297) (1997) 218–220, https://doi.org/10.1126/science.275.5297.218.

[24] D.R. Valenzano, E. Terzibasi, T. Genade, A. Cattaneo, L. Domenici, A. Cellerino, Resveratrol prolongs lifespan and retards the onset of age-related markers in a short-lived vertebrate, Curr. Biol. 16 (3) (2006) 296–300, https://doi.org/10.1016/j.cub.2005.12.038.

[25] J.H. Li, Z.W. Zhong, J.R. Yuan, X.H. Chen, Z.Y. Huang, Z.Y. Wu, Resveratrol improves endothelial dysfunction and attenuates atherogenesis in apolipoprotein E-deficient mice, JNB (J. Nutr. Biochem.) 67 (2019) 63–71, https://doi.org/10.1016/j.jnutbio.2019.01.022.

[26] K.A.O. Gandy, J.J. Zhang, P. Nagarkatti, M. Nagarkatti, Resveratrol (3, 5, 4'-Trihydroxy-trans-Stilbene) attenuates a mouse model of multiple sclerosis by altering the miR-124/sphingosine kinase 1 Axis in encephalitogenic T cells in the brain, J. Neuroimmune Pharmacol. 14 (3) (2019) 462–477, https://doi.org/10.1007/s11481-019-09842-5.

[27] S.F. Ahmad, M.A. Ansari, A. Nadeem, S.A. Bakheet, M.Z. Alzahrani, M.A. Alshammari, W.A. Alanazi, A.F. Alasmari, S.M. Attia, Resveratrol attenuates pro-inflammatory cytokines and activation of JAK1-STAT3 in BTBR T+ Itpr3(tf)/J autistic mice, Eur. J. Pharmacol. 829 (2018) 70–78, https://doi.org/10.1016/j.ejphar.2018.04.008.

[28] L. Cheng, Z.X. Jin, R. Zhao, K. Ren, C. Deng, S.Q. Yu, Resveratrol attenuates inflammation and oxidative stress induced by myocardial ischemia-reperfusion injury: role of Nrf2/ARE pathway, Int. J. Clin. Exp. Med. 8 (7) (2015) 10420–10428.

[29] W.W. Dong, Y.J. Liu, Z. Lv, Y.F. Mao, Y.W. Wang, X.Y. Zhu, L. Jiang, Lung endothelial barrier protection by resveratrol involves inhibition of HMGB1 release and HMGB1-induced mitochondrial oxidative damage via an Nrf2-dependent mechanism, Free Radic. Biol. Med. 88 (2015) 404–416, https://doi.org/10.1016/j.freeradbiomed.2015.05.004.

[30] C.W. Chen, Y.M. Li, S.Y. Hu, W. Zhou, Y.X. Meng, Z.Z. Li, Y. Zhang, J. Sun, Z. Bob, M.L. DePamphilis, Y. Yen, Z.Y. Han, W.G. Zhu, DHS (trans-4,4 '-dihydroxystilbene) suppresses DNA replication and tumor growth by inhibiting RRM2 (ribonucleotide reductase regulatory subunit M2), Oncogene 38 (13) (2019) 2364–2379, https://doi.org/10.1038/s41388-018-0584-6.

[31] M. Savio, D. Ferraro, C. Maccario, R. Vaccarone, L.D. Jensen, F. Corana, B. Mannucci, L. Bianchi, Y.H. Cao, L.A. Stivala, Resveratrol analogue 4,4 '-dihydroxy-trans-stilbene potently inhibits cancer invasion and metastasis, Sci. Rep. 6 (2016), https://doi.org/10.1038/srep19973.

[32] P. Torres, J. Guillermo Avila, A. Romo de Vivar, A.M. García, J.C. Marín, E. Aranda, C.L. Céspedes, Antioxidant and insect growth regulatory activities of stilbenes and extracts from Yucca periculosa, Phytochemistry 64 (2) (2003) 463–473, https://doi.org/10.1016/S0031-9422(03)00348-0.

[33] W. Chen, S.C.M. Yeo, M.G.A.A. Elhennawy, X.Q. Xiang, H.S. Lin, Determination of naturally occurring resveratrol analog trans-4,4'-dihydroxystilbene in rat plasma by liquid chromatography-tandem mass spectrometry: application to a pharmacokinetic study, Anal. Bioanal. Chem. 407 (19) (2015) 5793–5801, https://doi.org/10.1007/s00216-015-8762-7.

[34] B.M. Fischer, E. Pavlisko, J.A. Voynow, Pathogenic triad in COPD: oxidative stress, protease-antiprotease imbalance, and inflammation, Int. J. Chronic Obstr. Pulm. Dis. 6 (2011) 413–421, https://doi.org/10.2147/COPD.S10770.

[35] A. Kobayashi, M.I. Kang, Y. Watai, K.I. Tong, T. Shibata, K. Uchida, M. Yamamoto, Oxidative and electophilic stresses activate Nrf2 through inhibition of ubiquitination activity if Keap1, Mol. Cell. Biol. 26 (1) (2006) 221–229, https://doi.org/10.1128/MCB.26.1.221-229.2006.

[36] T. Satoh, S.I. Okamoto, J. Cui, Y. Watanabe, K. Furuta, M. Suzuki, K. Tohyama, S.A. Lipton, Activation of the Keap1/Nrf2 pathway for neuroprotection by electrophillic phase II inducers, Proc. Natl. Acad. Sci. U.S.A. 103 (3) (2006) 768–773, https://doi.org/10.1073/pnas.0505723102.

[37] D.D. Zhang, M. Hannink, Distinct cysteine residues in Keap1 are required for Keap1-dependent ubiquitination of Nrf2 and for stabilization of Nrf2 by chemopreventive agents and oxidative stress, Mol. Cell. Biol. 23 (22) (2003) 8137–8151, https://doi.org/10.1128/MCB.23.22.8137-8151.2003.

[38] N. Wakabayashi, A.T. Dinkova-Kostova, W.D. Holtzclaw, M.I. Kang, A. Kobayashi, M. Yamamoto, T.W. Kensler, P. Talalay, Protection against electrophile and oxidant stress by induction of the phase 2 response: fate of cysteines of the Keap1 sensor modified by inducers, Proc. Natl. Acad. Sci. U.S.A. 101 (7) (2004) 2040–2045, https://doi.org/10.1073/pnas.0307301101.

[39] M. Kobayashi, L. Li, N. Iwamoto, Y. Nakajima-Takagi, H. Kaneko, Y. Nakayama, M. Eguchi, Y. Wada, Y. Kumagai, M. Yamamoto, The antioxidant defense system keap1-Nrf2 comprises a multiple sensing mechanism for responding to a wide range of chemical compounds, Mol. Cell. Biol. 29 (2) (2009) 493–502, https://doi.org/10.1128/MCB.01080-08.

[40] J.L. Wright, A. Churg, Animal models of cigarette smoke-induced COPD, Chest 122 (6) (2002) 301S–306S, https://doi.org/10.1378/chest.122.6_suppl.301S.

[41] A. Churg, M. Cosio, J.L. Wright, Mechanisms of cigarette smoke-induced COPD: insights from animal models, Am. J. Physiol. Lung Cell Mol. Physiol. 294 (4) (2008) L612–L631, https://doi.org/10.1152/ajplung.00390.2007.

[42] A. Tamimi, D. Serdarevic, N.A. Hanania, The effects of cigarette smoke on airway inflammation in asthma and COPD: therapeutic implications, Respir. Med. 106 (3) (2012) 319–328, https://doi.org/10.1016/j.rmed.2011.11.003.

[43] S. Rajendrasozhan, S.R. Yang, I. Edirisinghe, H.W. Yao, D. Adenuga, I. Rahman, Deacetylases and NF-kappa B in redox regulation of cigarette smoke-induced lung inflammation: epigenetics in pathogenesis of COPD, Antioxidants Redox Signal. 10 (4) (2008) 799–811, https://doi.org/10.1089/ars.2007.1938.

[44] G. Krommidas, K. Kostikas, G. Papatheodorou, A. Koutsokera, K.I. Gourgoulianis, C. Roussos, N.G. Koulouris, S. Loukides, Plasma leptin and adiponectin in COPD exacerbations: associations with inflammatory biomarkers, Respir. Med. 104 (1) (2010) 40–46, https://doi.org/10.1016/j.rmed.2009.08.012.

[45] M. Profita, G. Chiappara, F. Mirabella, R. Di Giorgi, L. Chimenti, G. Costanzo, L. Riccobono, V. Bellia, J. Bousquet, A.M. Vignola, Effect of cilomilast (Ariflo) on TNF-alpha, IL-8, and GM-CSF release by airway cells of patients with COPD, Thorax 58 (7) (2003) 573–579, https://doi.org/10.1136/thorax.58.7.573.

[46] J.J. Sng, S. Prazakova, P.S. Thomas, C. Herbert, MMP-8, MMP-9 and neutrophil elastase in peripheral blood and exhaled breath condensate in COPD, COPD 14 (2) (2017) 238–244, https://doi.org/10.1080/15412555.2016.1249790.

[47] M.Q. Mahmood, D. Reid, C. Ward, H.K. Muller, D.A. Knight, S.S. Sohal, E.H. Walters, Transforming growth factor (TGF) beta(1) and Smad signalling pathways: a likely key to EMT-associated COPD pathogenesis, Respirology 22 (1) (2017) 133–140, https://doi.org/10.1111/resp.12882.

[48] S.L. Dallas, J.L. Rosser, G.R. Mundy, L.F. Bonewald, Proteolysis of latent transforming growth factor-beta (TGF-beta)-binding protein-1 by osteoclasts - a cellular mechanism for release of TGF-beta from bone matrix, J. Biol. Chem. 277 (24) (2002) 21352–21360, https://doi.org/10.1074/jbc.M111663200.

[49] S.S. Tao, Y. Zheng, A. Lau, M.C. Jaramillo, B.T. Chau, R.C. Lantz, P.K. Wong, G.T. Wondrak, D.D. Zhang, Tanshinone I activates the Nrf2-dependent antioxidant response and protects against as(III)-Induced lung inflammation in vitro and in vivo, Antioxidants Redox Signal. 19 (14) (2013) 1647–1661, https://doi.org/10.1089/ars.2012.5117.

[50] Y. Ishii, K. Itoh, Y. Morishima, T. Kimura, T. Kiwamoto, T. Ilzuka, A.E. Hegab, T. Hosoya, A. Nomura, T. Sakamoto, M. Yamamoto, K. Sekizawa, Transcription factor Nrf2 plays a pivotal role in protection against elastase-induced and emphysema, J. Immunol. 175 (10) (2005) 6968–6975, https://doi.org/10.4049/jimmunol.175.10.6968.

[51] M.C. Lu, J. Zhao, Y.T. Liu, T. Liu, M.M. Tao, Q.D. You, Z.Y. Jiang, A potent inhibitor of the Keap1-Nrf2 protein-protein interaction, alleviates renal inflammation in mice by restricting oxidative stress and NF-kappaB activation, Redox Biol. 26 (2019) 101266, https://doi.org/10.1016/j.redox.2019.101266 CPUY192018.

[52] N. Li, A.E. Nel, Role of the Nrf2-mediated signaling pathway as a negative regulator of inflammation: implications for the impact of particulate pollutants on asthma, Antioxidants Redox Signal. 8 (1–2) (2006) 88–98, https://doi.org/10.1089/ars.2006.8.88.

[53] S. Ruiz, P.E. Pergola, R.A. Zager, N.D. Vaziri, Targeting the transcription factor Nrf2 to ameliorate oxidative stress and inflammation in chronic kidney disease, Kidney Int. 83 (6) (2013) 1029–1041, https://doi.org/10.1038/ki.2012.439.

[54] E.H. Kobayashi, T. Suzuki, R. Funayama, T. Nagashima, M. Hayashi, H. Sekine, N. Tanaka, T. Moriguchi, H. Motohashi, K. Nakayama, M. Yamamoto, Nrf2 suppresses macrophage inflammatory response by blocking proinflammatory cytokine transcription, Nat. Commun. 7 (2016), https://doi.org/10.1038/ncomms11624.